Acute Effects of Mitoxantrone on the Electromechanical Properties of Ventricular Myocardium

Dissertation

zur Erlangung des Doktorgrades im Fachbereich Chemie

der Universität Hamburg

vorgelegt von

Gexin Wang

aus Shanghai

Hamburg 2000

Gutachter: Prof. Dr. H.-J. Duchstein
Prof. Dr. M. Korth

Mündliche Prüfung: 27. Juni 2000

Contents

1. Introduction

1.1 Clinical values of the anticancer drugs with anthraquinone structure

Anthraquinone-based antitumor drugs can be divided into two classes according to their structural characteristics and their origin: (1) anthracycline antibiotics such as doxorubicin (Figure 1) which are isolated from cultures of *Streptomyces peucetius* var. *caesius*; (2) synthetic anthracenedione derivatives such as mitoxantrone (MTO) (Figure 1). Anthracycline antibiotics have long been proven to be highly effective anticancer drugs which are widely used in the treatment of acute leukemias, malignant lymphomas and a variety of solid tumors (Young et al., 1981). The therapeutic use of these drugs, however, is limited by their cardiotoxic effects which include various types of arrhythmia and life-threatening cardiomyopathy (Kantrowitz and Bristow, 1984; Rhoden et al., 1993; Singal and Iliskovic,

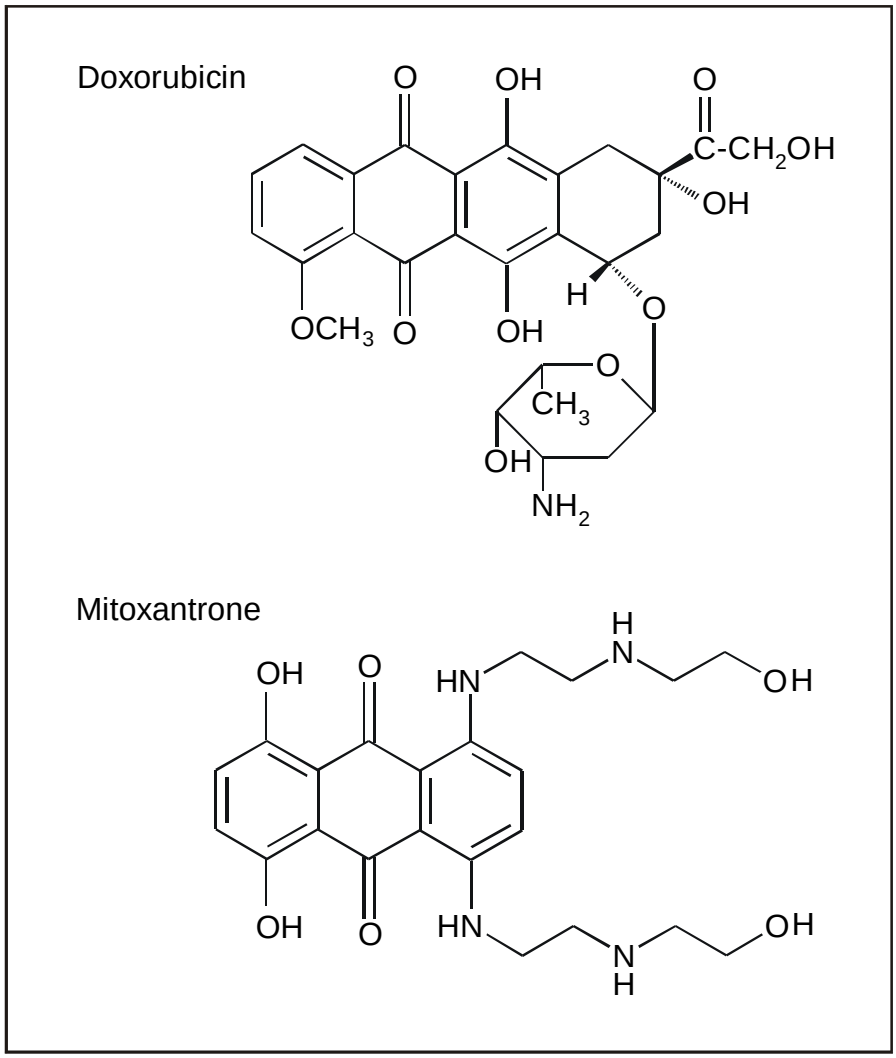

Figure 1. Chemical structures of doxorubicin and mitoxantrone

1998). MTO, or 1,4-dihydroxy-5,8-bis{{2-[(2-hydroxyethyl)-amino]ethyl}-amino}-9,10-anthracenedione dihydrochloride, was developed in an attempt to circumvent the cardiotoxicity associated with doxorubicin (Johnson et al., 1979; Murdock et al., 1979). MTO has antitumor activity similar to doxorubicin in animal tumor models (Wallace et al., 1979). Clinically, MTO applied either as a single agent or as a component of combination treatment regimens has demonstrated therapeutic efficacy in patients with a wide range of solid tumors such as advanced breast cancer, non-Hodgkin's lymphoma and several forms of leukemia (Shenkenberg and von Hoff, 1986; Weiss, 1989; Faulds et al., 1991). Like anthracycline antibiotics, the antitumor effects of MTO result mainly from the blockade of DNA synthesis which may be caused by: (1) intercalation of MTO between base pairs of DNA in actively cycling cells; (2) inhibition of the DNA topoisomerase II by MTO (Shenkenberg and von Hoff, 1986; Malonne and Atassi, 1997). MTO has demonstrated considerably better tolerability than anthracycline antibiotics with regard to the severity of nausea, vomiting, stomatitis, alopecia and cardiotoxicity (Neidhart et al., 1986; Henderson et al., 1989), but contrary to what was initially thought, adverse cardiac effects have also been clearly documented with MTO (Shenkenberg and von Hoff, 1986; Faulds et al., 1991; Benjamin, 1995).

1.2 Cardiac toxic effects of anthracyclines and mitoxantrone

1.2.1 Animal studies

As the prototype of anthracyclines, doxorubicin has been most extensively investigated in animal experiments regarding the cardiotoxicity (Olson and Mushlin, 1990). Doxorubicin has also been regularly used as a reference compound in the experimental study of cardiotoxic effects of MTO. In general, comparative studies on animal models revealed similar pathological changes of myocardial structure and contractile function induced by MTO and doxorubicin, although some experiments showed a much less severe myocardial damage caused by MTO as compared to that of doxorubicin.

In early experiments on beagle dogs comparing the cardiotoxicity of doxorubicin and MTO, abnormalities of electrocardiograms and lethal congestive heart failure were observed in doxorubicin-treated animals; however, no such changes were seen in any dogs given MTO (Henderson et al., 1982). Endomyocardial biopsy samples from dogs during treatment with doxorubicin revealed progressive cardiomyopathy, but these changes were absent in MTO-treated dogs. The only ultrastructural alteration induced by MTO was dilatation of the sarcoplasmic reticulum (Sparano et al., 1982).

In other animal models, MTO did produce significant myocardial changes. A dose-related impairment of cardiac contractility induced by MTO has been shown in the isolated and perfused rabbit heart (Tumminello et al., 1987). In one report, MTO induced doxorubicin-like focal myocardial damage in a mouse model and functionally reduced right atrial response to histamine in guinea pigs (Perkins et al., 1984). A later study using a chronic mouse model confirmed the myocardial damage caused by MTO (Alderton et al., 1992). Cardiac tissues obtained from MTO-treated mice displayed mitochondria swelling, vacuolation and swelling of the cisternae of the sarcoplasmic reticulum, dilation of the t-tubular system and slight myofibrillar lysis. These ultrastructural changes were comparable to those induced by doxorubicin, although the proportion of myocytes showing these alterations was smaller in comparison to the doxorubicin-treated cell. Similar myocardial lesions were also demonstrated in spontaneously hypertensive rats chronically treated with MTO (Herman et al., 1997). The severity of MTO-induced cardiomyopathy in these rats was dose-dependent.

1.2.2 Clinical manifestations

Cardiotoxic effects associated with anthracycline chemotherapy have been regularly documented in clinical studies (Blum and Carter, 1974; Kantrowitz and Bristow, 1984; Rhoden and Hasleton, 1993; Singal and Iliskovic, 1998). Anthracyclines can cause acute cardiotoxic effects such as tachycardia, dysrhythmias and even sudden death (von Hoff et al, 1977; Wortman et al., 1979; Steinberg et al., 1987). The main delayed cardiotoxicity related to anthracycline treatment includes cardiomyopathy and congestive heart failure which become more frequent and severe when cumulative doses of doxorubicin increased (Lefrak et al., 1973; von Hoff et al., 1979).

Similar to that of anthracycline antibiotics, the clinical manifestations of cardiotoxicity of MTO can be divided into two categories: (a) acute effects manifested by cardiac arrhythmias, and (b) a chronic effect in form of decreased ventricular function which may ultimately lead to congestive heart failure.

Electrocardiographic changes seen during MTO therapy include non-specific ST-T wave changes or T-wave abnormalities and atrial or ventricular arrhythmias (Posner et al., 1985). One clinical study reported that 5 individuals in a cohort of 766 cancer patients developed significant arrhythmias such as atrial or ventricular fibrillation while receiving MTO treatment (Gams and Wesler, 1984). Myocardial infarction associated with MTO also occurred in some patients (Clark et al., 1984; Gams and Wesler, 1984).

Reduction in left ventricular ejection fraction related to MTO therapy has been regularly observed in clinical trials (Shenkenberg and von Hoff, 1986; Henderson et al., 1989; Wiseman and Spencer, 1997). Some patients even experienced congestive heart failure with MTO. The incidence of congestive heart failure is dependent on the cumulative dose of MTO (Clark et al., 1984). Histopathologic changes typical of anthracycline cardiotoxicity have also been demonstrated on endomyocardial biopsy from patients treated with MTO, although these changes appear to be less severe than that induced by doxorubicin (Benjamin, 1995). The observed ultrastructural alterations include tubular swelling, myofibrillar lysis, minimal chromatin clumping, and degeneration of mitochondria (Unverferth et al., 1983).

Risk factors for the MTO-associated cardiotoxicity include previous anthracycline therapy, mediastinal irradiation and a history of cardiovascular diseases (Faulds et al., 1991). Patients older than 70 years of age seemed to be more vulnerable to MTO-related cardiotoxicity (Benjamin, 1995).

1.3 Possible mechanisms of anthracycline and mitoxantrone cardiotoxicity

During the last two decades, various experimental approaches have been used in scientific research for a better understanding of the mechanisms of cardiotoxic effects induced by anthracyclines and MTO. These studies indicated that cardiotoxicity of anthracyclines and MTO is not mediated by the same mechanisms as those underlying the antitumor effects of these drugs, i.e., DNA intercalation and the inhibition of DNA topoisomerase II (Olson and Mushlin, 1990; Singal et al., 1997; Minotti et al., 1999). Based on the observed cellular and molecular actions of doxorubicin on myocardium, various hypotheses have been put forward to explain the cardiotoxicity of anthracyclins (Olson and Mushlin, 1990); the prevailing hypotheses include: (1) free radical formation; (2) disturbance of calcium homeostasis. These two hypotheses have also been tested for MTO.

1.3.1 Free radical and iron hypothesis

According to the free radical and iron hypothesis, the one-electron redox cycling of the quinone moiety and/or of the iron complex of anthracycline is able to generate superoxide, hydrogen peroxide and the extremely reactive hydroxyl radical which may cause cell damage by oxidizing lipid membranes, proteins and DNA. (Myers et al., 1986; Powis, 1989; Ryan and Aust, 1992). In addition to its ability to generate reactive oxygen species, anthracycline semiquinones can also release iron from the cellular iron storage protein, ferritin, thus further facilitate the formation of hydroxyl radical (Minotti, 1993).

In most cells, the chance for the formation of hydroxyl radical is kept to a minimum by the presence of detoxifying enzymes (e.g., superoxide dismutase, catalase and glutathione peroxidase). Consistent with the free radical and iron hypothesis, cardiomyocytes are poorly equipped with these enzymes and thus may provide the ideal place for the formation of hydroxyl radical (Olson et al., 1981). Other evidence supporting the free radical and iron hypothesis came from the preclinical and clinical trials showing that iron chelator (e.g., dexrazoxane) can partially protect the heart from anthracycline-induced short-term damage both in animal models and in patients during anthracycline therapy (Speyer et al., 1988; Dorr, 1996). On the other hand, controversy arouse from studies with antioxidants. Whereas antioxidants such as vitamin E and N-acetylcysteine proved to be effective in ameliorating anthracycline-induced myocardial damage (Dorr, 1996), no such protective effects could be demonstrated in large animal models of anthracycline cardiotoxicity (van Vleet et al., 1980; Herman et al., 1985) or in patients during doxorubicin therapy (Legha et al., 1982; Myers et al, 1983). These conflicting results with antioxidants imply that the free radical and iron hypothesis can not fully explain the anthracycline cardiotoxicity.

Compared with doxorubicin, MTO also contains quinone moiety and the structure necessary for the formation of iron complex. Thus, it was believed that free radicals and iron may also be involved in the cardiotoxicity of MTO. Several experimental studies have been carried out to test this assumption. In cardiac sarcoplasmic reticulum and submitochondrial particles or mitochondrial NADH dehydrogenase preparation, doxorubicin stimulated generation of superoxide, hydrogen peroxide and hydroxyl radical, whereas no such effects were detected with MTO (Doroshow and Davies, 1983; Doroshow, 1983). More surprisingly, in contrast to doxorubicin, MTO has been shown to inhibit the basal and drug-stimulated lipid peroxidation in a variety of subcellular systems including cardiac sarcosomes and mitochondria (Kharasch and Novak, 1983). The attenuation of fatty acid peroxidation by MTO may results from an inhibition of H_2O_2-dependent initiation and propagation reactions (Kharasch and Novak, 1985). In a mouse model treated with doxorubicin or MTO, the endogenous lipid peroxidation rate in heart tissue was not influenced by MTO, but was increased by doxorubicin (Arnaiz and Llesuy, 1993). The role of iron in the MTO cardiotoxicity has been tested in a chronic mouse model (Alderton et al., 1992). It was shown that the iron chelator dexrazoxane could protect the heart from damage induced by doxorubicin, but not by MTO. However, a later study, using cultured neonatal rat cardiac cells as a acute test system, demonstrated that dexrazoxane provided partial protection from MTO cardiotoxicity (Shipp et al., 1993). Taken together,

most investigations so far did not suggest a significant role of the free radicals in the cardiotoxicity of MTO.

1.3.2 Ca^{2+} hypothesis

Disturbance of intracellular Ca^{2+} homeostasis has long been suggested to play an important role in the anthracycline cardiotoxicity. Early studies revealed substantial accumulations of Ca^{2+} in ventricular myocardium and excessive Ca^{2+} inclusions in mitochondria after the treatment with doxorubicin, suggesting that anthracycline-induced cardiomyopathy may be caused by overload of the intracellular Ca^{2+} (Olson et al, 1974; Revis and Marusic, 1979; Singal et al, 1983). The Ca^{2+} overload hypothesis was then challenged by several other studies. Jensen et al. (1986) proposed that doxorubicin-induced cardiac dysfunction is associated with a deficiency rather than an excess of intracellular calcium. In their study, papillary muscles isolated from rats chronically treated with doxorubicin exhibited decreased contractility. Unlike what might be expected if anthracyclins caused a Ca^{2+} overloaded state, elevation of Ca^{2+} concentration in the bath solution increased contraction more in doxorubicin-treated than in control papillary muscles. Similar results were observed in a rabbit Langendorff heart preparation (Rabkin, 1983). In this same study, doxorubicin caused a significant reduction in the velocity of the ventricular pressure development during the contraction, suggesting that the function of the cardiac sarcoplasmic reticulum (SR) may be affected by doxorubicin.

The SR plays an important role in the regulation of cytoplasmic Ca^{2+} concentration and, thereby, the contraction-relaxation cycle of the cardiac muscle (Bers, 1992). Release of Ca^{2+} from the SR induced by influx of Ca^{2+} through sarcolemmal Ca^{2+} channels during membrane excitation triggers contraction (Fabiato, 1985), whereas active Ca^{2+} reuptake by the SR contributes to relaxation (Bassani et al., 1994). The evidence for a direct interference of doxorubicin with SR function was provided by studies using isolated SR preparations. The first experiment which clearly showed that doxorubicin triggers Ca^{2+} release from SR was carried out in a highly purified SR fraction from rabbit skeletal muscle (Zorzato et al., 1985). The results demonstrated that this effect was not associated with the production of semiquinone, and it was proposed that doxorubicin selectively activated a Ca^{2+} efflux pathway in the SR. A similar effect was also observed in SR vesicles isolated from canine heart (Kim et al., 1989). These results were further supported by studies addressing the interactions between doxorubicin and SR Ca^{2+} release channels. In a skeletal muscle preparation, doxorubicin was shown to interact specifically with the ryanodine receptor

complex, which is part of the SR Ca^{2+} release channel (Abramson et al., 1988). By incorporating purified skeletal SR Ca^{2+} release channels into lipid bilayers, Nagasaki and Fleischer (1989) was able to demonstrate that doxorubicin directly activates the Ca^{2+} release channels by increasing the channel open probability. These observations in skeletal preparations were confirmed by experiments using cardiac membrane vesicles enriched in SR (Holmberg and Williams, 1990; Pessah, et al., 1990), or isolated cardiac SR Ca^{2+} release channels (Holmberg and Williams, 1990; Ondrias et al., 1990). When the acute effects of doxorubicin were investigated in functionally intact guinea-pig cardiomyocytes, an impaired Ca^{2+}-induced Ca^{2+} release from SR during excitation was manifested by a significant decrease in the velocity of the rising phase of intracellular Ca^{2+} transient (Wang and Korth, 1995). This phenomenon is as expected, since a doxorubicin-induced persistent opening of the SR Ca^{2+} release channel can attenuate the ability of SR to accumulate Ca^{2+} (Halili-Rutman et al.,1997), and hence, reduce the SR Ca^{2+} release in response to a normal action potential. In a chronic rabbit model treated with doxorubicin, the density of the cardiac SR Ca^{2+} release channels was significantly reduced (Dodd et al., 1993). The magnitude of the decrease in cardiac SR Ca^{2+} release channel density was correlated with the severity of the cardiomyopathy. Thus, the pathogenesis of anthracycline cardiotoxicity appears to involve both an altered function and a decreased density of the SR Ca^{2+} release channels.

The interaction of MTO with SR Ca^{2+} release channels is complex. By using skeletal muscle SR vesicles and chemically skinned psoas muscle fibers, Abramson et al. (1988) demonstrated that MTO at low concentration (≤10 μM) is a potent stimulator of Ca^{2+} efflux from SR. To elucidate the molecular mechanism of MTO-induced SR Ca^{2+} release, Holmberg and Williams (1990) investigated directly the action of MTO on purified cardiac SR Ca^{2+} release channels in artificial phospholipid bilayers. At low concentrations (1-10 μM), MTO increased single channel open probability. However, when the drug concentration was increased, a decreased open probability associated with longer opening events was observed. The specific [^{3}H]ryanodine binding to SR vesicles isolated from sheep hearts was also inhibited by high concentration of MTO. Since [^{3}H]ryanodine binds to the channel only in its open state, high concentration of MTO seems to keep the Ca^{2+} release channels in the closed state. Even more complicated, Kim et al. (1994) showed that MTO and doxorubicin exhibited antithetical activities towards the ryanodine receptor. Under conditions promoting channel closure, doxorubicin markedly enhanced the binding of [^{3}H]ryanodine, whereas MTO had very low efficacy towards activating the binding of [^{3}H]ryanodine. Unlike doxorubicin, MTO assayed under conditions promoting channel opening inhibited the binding of [^{3}H]ryanodine.

When both drugs were present in combination, MTO competitively antagonized the ability of doxorubicin to activate the ryanodine receptor. Furthermore, MTO per se did not alter active Ca^{2+} accumulation by SR but fully inhibited doxorubicin-induced Ca^{2+} release. The above results suggest that MTO differ from doxorubicin in its action on the SR Ca^{2+} release channels.

2. Aim of the study

As has been discussed above, although the acute and chronic cardiotoxicity of MTO has been clearly described in clinical studies, its cellular and molecular mechanisms remain to be clarified. The purpose of the present study was to investigate the acute effects of MTO on electrophysiological and contractile processes of cardiac myocytes, and thereby to gain more insight into the cellular mechanisms responsible for the cardiotoxicity of MTO. As a model, the guinea-pig heart preparations were regularly used in this study. Some experiments were carried out on rat or human cardiac preparations. The focus of the study has been set on the influence of MTO on the excitation-contraction coupling in isolated guinea-pig ventricular preparations.

The experiments were divided into three parts. In the first part, the effects of MTO on action potentials and various types of membrane currents were determined by using intracellular microelectrode recording and whole-cell patch-clamp techniques. The second part of experiments concentrated on the effect of MTO on cardiac muscarinic receptors. Indirect analysis using membrane currents as functional probes as well as direct radioligand binding assay were utilized to identify the interaction of MTO with muscarinic receptors. In the third part of experiments, the effects of MTO on myocardial contraction were investigated in isolated multicellular preparations (papillary muscles) and ventricular myocytes. The methods applied were the isometric contraction recording, the whole-cell patch-clamp method in combination with a cell-edge detecting technique and fluorescencemicroscopy for the quantification of intracellular Ca^{2+} concentration.

3. Methods

3.1 Preparation of right ventricular papillary muscles

Guinea pigs of either sex weighing 250 to 350 g were anaesthetized with ether or halothan and subsequently killed by cervical dislocation. After opening the thorax, the heart was rapidly removed and transferred into a pre-warmed modified Krebs-Henseleit solution vigorously gassed with 95% O_2 and 5% CO_2. Right ventricular papillary muscles (diameter, 0.5 to 0.8 mm), with the tendons attached to them, were carefully excised from the isolated heart and mounted in a two-cambered organ bath with internal circulation of the modified Krebs-Henseleit solution (volume, 50 ml). The bath solution was constantly gassed and kept in circulation by 95% O_2 and 5% CO_2; the temperature was maintained at 35^{o}C by a thermostat. The modified Krebs-Henseleit solution had the following composition (in mM): NaCl 115, KCl 4.7, $MgSO_4$ 1.2, $CaCl_2$ 2.0, $NaHCO_3$ 25, KH_2PO_4 1.2, and glucose 10. The pH of the solution was 7.4.

3.2 Contraction measurement in papillary muscles

The papillary muscles were mounted vertically, with their basal end fixed by a stainless-steel clamp and their tendon connected to a force transducer. The muscles were stimulated at their base through two punctate platinum electrodes with square-wave pulses of 2 ms in duration and an intensity 10% above threshold. To suppress the stimulation-evoked release of endogenous catecholamines, all experiments were performed in the presence of 20 nM tetrodotoxin (TTX), which blocks Na^+ channels of nerve endings (the exocytotic release of endogenous catecholamines depends on the depolarization of sympathetic nerve endings in the heart), but has almost no effects on the electrical and mechanical properties of myocardial cells (Honerjäger, 1982; Sakakibara et al., 1993). The force of contraction was measured isometrically by means of an inductive force transducer (Q-11, 10p, Hottinger Baldwin Meßtechnik, Germany) connected to an oscilloscope and a digital audio tape recorder (DAT-recorder DTR-1202, Bio-Logic, France). Each muscle was stretched to reach a resting tension of 4 mN. At this resting tension the force of contraction produced by the muscles was approximately maximal under the present experimental conditions. The resting tension was kept constant throughout the experiment. An equilibration period of at least 1 h at a stimulation frequency of 1 Hz preceded each experiment. Subsequently, the frequency of stimulation was lowered to 0.5 Hz, and the drug intervention was started as soon as the force

of contraction had reached a steady state. The following parameters of the isometric contraction were evaluated: peak force of contraction, time to peak force and relaxation time (measured at 90% of relaxation).

3.3 Action potential measurement in papillary muscles

Papillary muscles were mounted horizontally in the bath and stimulated via two punctate platinum electrodes with square-wave pulses of 2 ms in duration and an intensity 10% above threshold. Transmembrane electrical activity was recorded with conventional glass microelectrodes. The microelectrodes were made of borosilicate glass capillaries (TW-150F-4, World Precision Instrument, New Haven, CT, U.S.A.). The capillaries were heated and pulled by an electrode-puller (DMZ-Universal Puller, München, Germany) into two parts, each with a fine open tip <1 µm in diameter. The lumen of the microelectrodes was filled with filtered 3 M KCl and connected to a Ag-AgCl half-cell via an microelectrode holder. The tip resistances of the microelectrodes ranged from 10 to 20 MΩ. The impalement of the cells with the microelectrode was achieved via a micromanipulator (Leitz, Wetzlar, Germany). Membrane potentials were measured by means of an electrometer amplifier (model 773, World Precision Instruments), and the signals were stored on a DAT-recorder (DTR-1202, Bio-Logic, France) and subsequently evaluated by a computer. The maximum rate of rise of the action potential (V_{max}) was obtained by an electronic differentiator with linear differentiation in the range 0 to 1000 V/s. Only experiments with microelectrode impalement lasting throughout the entire experimental period were accepted for evaluation.

3.4 Isolation of cardiac myocytes

Cardiac myocytes were prepared from ventricles or atria of adult guinea pigs or rats by enzymatic dissociation according to Powell *et al*. (1980) with some modifications. The animals were anaesthetized with ether or halothane and subsequently killed by cervical dislocation. After opening the chest, the heart was excised, with a section of the aorta (about 4 mm) attached to it, and put into a modified Krebs-Henseleit solution gassed with 95% O_2 and 5% CO_2. After quickly trimming away other tissues, the heart was connected via the aorta to a Langendorff perfusion apparatus. The heart was retrogradely perfused at 37°C and at a constant rate of 10 ml/min with the following solutions: 5 minutes with a nominally Ca^{2+}-free Joklik-MEM solution (Biochrom; see Table 1 for the composition) and then, 5-15 minutes with the same solution to which had been added 50 µM $CaCl_2$, collagenase (Worthington type II, 25 mg/50 ml, Biochrom), protease (type XIV, 10 mg/50 ml, Sigma), and 0.1% bovine

serum albumin (fraction V, Sigma). All solutions were gassed with 5% CO_2 in O_2; the pH was 7.4. After perfusion, the ventricles or the atria were separated, minced and incubated in fresh enzyme solution at 37^{o}C for 5-10 min. The myocytes were then disaggregated by gentle mechanical agitation. After filtration through a nylon mesh, the cells were centrifuged at 37g for 3 minutes and then resuspended in Joklik-MEM solution containing 300 μM $CaCl_2$ and 1% bovine serum albumin. The cell suspension was kept at room temperature under a continuous stream of 5% CO_2 in O_2 and used for experiments within 6 h after isolation. Usually, the yield of Ca^{2+}-tolerant rod-shaped ventricular myocytes with clear cross striation was 50-80% (Figure 2). The yield of relaxed atrial myocytes was 40-70%.

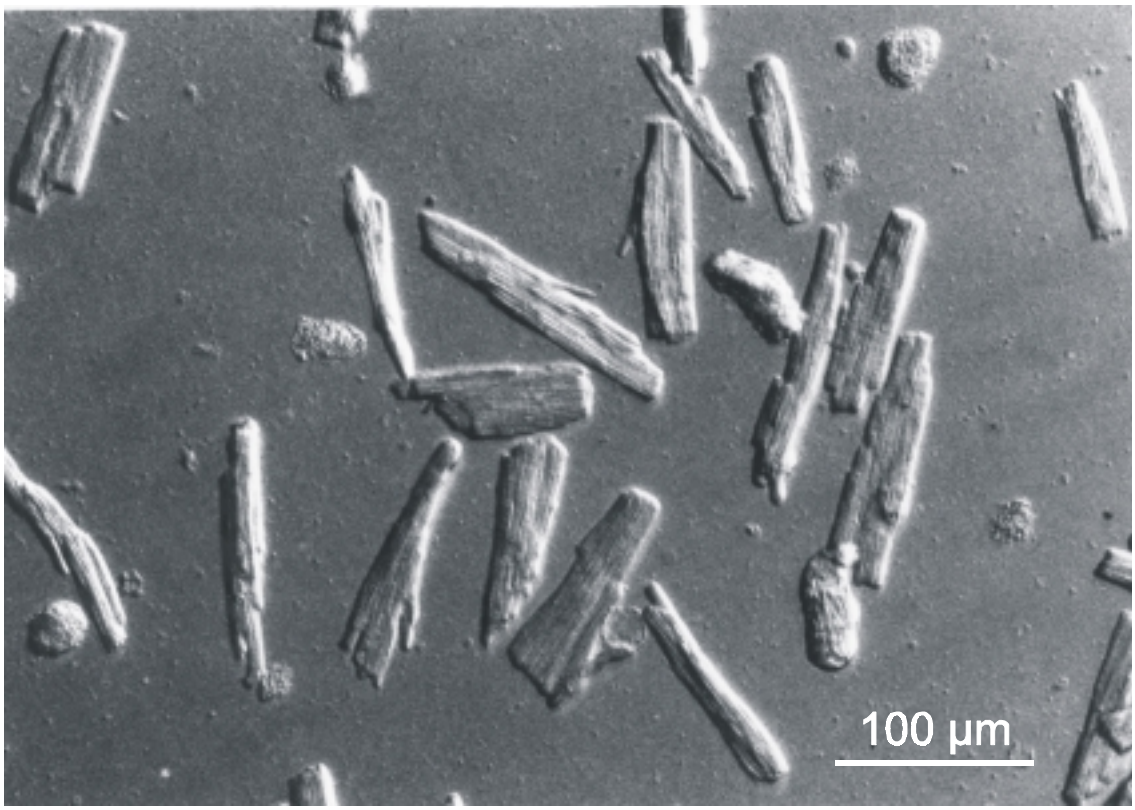

Figure 2. Typical appearance of the enzymatically isolated guinea-pig ventricular myocytes under light microscope. Myocytes that have rod shape and display clear cross striation were chosen for experiments. Granulated cells are those which were damaged during isolation procedure.

Table 1. Composition of Joklik modification of Minimum Essential Medium (Joklik-MEM).

Chemicals	mg/l	Chemicals	mg/l
KCl	400	L-methionine	15
$MgCl_2$ (anhydrous)	93.8	L-pheneylalanine	32
NaCl	6500	L-threonine	48
NaH_2PO_4	1327	L-tryptophane	10
$NaHCO_3$	2000	L-tyrosine-2Na	47
D-glucose	2000	L-valine	46
Phenol red	10	D-Ca-pantothenate	1
L-arginine	126	Choline chloride	1
L-cystine·$2H_2O$	32.4	Folic acid	1
L-glutamic acid	294	i-Inositol	2
L-histidine	31	Nicotinamide	1
L-isoleucine	52	Pyrodoxal·HCl	1
L-leucine	52	Riboflavin	0.1
L-lysine	58	Thiamine·HCl	1

Table 2. Composition of patch-electrode filling solutions for different measurements (mM).

Chemicals	Action potential Cell shortening Ca^{2+} transient	$I_{Ca\,(L)}$	I_{K1} $I_{backgroud}$ I_K & I_{Kr}	$I_{K,ACh}$
KCl	125		125	125
NaCl	5			
CsCl		125		
$MgSO_4$	2		2	2
K_2ATP	5		5	5
MgATP		5		
TEA-Cl		20		
EGTA		10	5	5
HEPES	5	5	5	5
GTP or GTP-γS				0.1
	pH 7.3 (with KOH)	pH 7.3 (with CsOH)	pH 7.3 (with KOH)	pH 7.3 (with KOH)

Before each experiment, a drop of cell suspension was added to a Tyrode solution in the recording chamber (volume, 0.5 ml) mounted on an inverted microscope (Axiovert 10, Carl Zeiss, Germany). The Tyrode solution contained (in mM): NaCl 138, $MgSO_4$ 1.2, $CaCl_2$ 2, KCl 5, glucose 10, HEPES 5; the pH was 7.4. After the cells had attached to the bottom, the bath was perfused at a flow rate of 4 ml/min with prewarmed Tyrode solution continuously gassed with O_2. A thermoprobe was placed near the cell, and the temperature in the bath (34^oC to 35^oC) was continuously controlled with a thermoelectric device (HFTC 15-3, NPI, Tamm, Germany). Only cells with clear cross striations and no membrane blebs were chosen for experiments.

3.5 Whole-cell patch-clamp technique

Patch-clamp experiments were performed in whole-cell configuration according to a method developed by Hamill et al (1981). Patch electrodes were fabricated from borosilicate glass capillaries (TW150F-4, World Precision Instruments) which were pulled by a electrode puller (DMZ-Universal Puller, München, Germany) in two stages into two separate parts, each with a tip openings of about 3 µm in diameter. The resistance of the patch electrodes ranged from 1.5 to 3 MΩ when filled with prefiltered electrode solutions of different composition (Table 2). The electrode was connected via an adapter to the probe of a patch-clamp amplifier (EPC7, List Medical Electronics, Germany). The probe was directly mounted on a three-dimensional hydraulic micromanipulator (MO-103M, Narishige, Japan).

For the formation of standard whole-cell configuration (Figure 3), the patch electrode was first moved down towards the cell, and the tip of the electrode was pressed against the cell surface to form a tight seal between electrode tip and membrane patch. After the resistance of the seal was increased into the gigaohm range via exertion of slight negative pressure in the electrode, the membrane patch under the electrode tip was ruptured by a short suction so that the whole-cell configuration was finally established.

To avoid possible loss of cytoplasmic diffusible components which may occur under standard whole-cell patch configuration, perforated whole-cell patch configuration (Horn and Marty, 198) (Figure 3) was used in some experiments. In this case, the membrane patch was not ruptured after formation of a gigaohm seal. Instead, the polyene antibiotic amphotericin B was used to permeabalize the membrane patch. Amphotericin B has the ability to form tiny pores in the membrane which enable a low-resistance electrical access to the cell interior, and allow passage of only small ions, thus preventing wash-out of intracellular macromolecules. Amphotericin B was first dissolved in DMSO (60 mg/ml), and then added to the electrode

filling solution to reach a final concentration of 300 µg/ml. An ultrasonicator was used to facilitate the solvation of amphotericin B. The process of perforation of the membrane patch was monitored by observing the change of the capacitative current in response to repetitive small voltage steps. Usually, 10-15 min were needed before the capacitative current increased to a stable level and series resistance reduced to <10 MΩ.

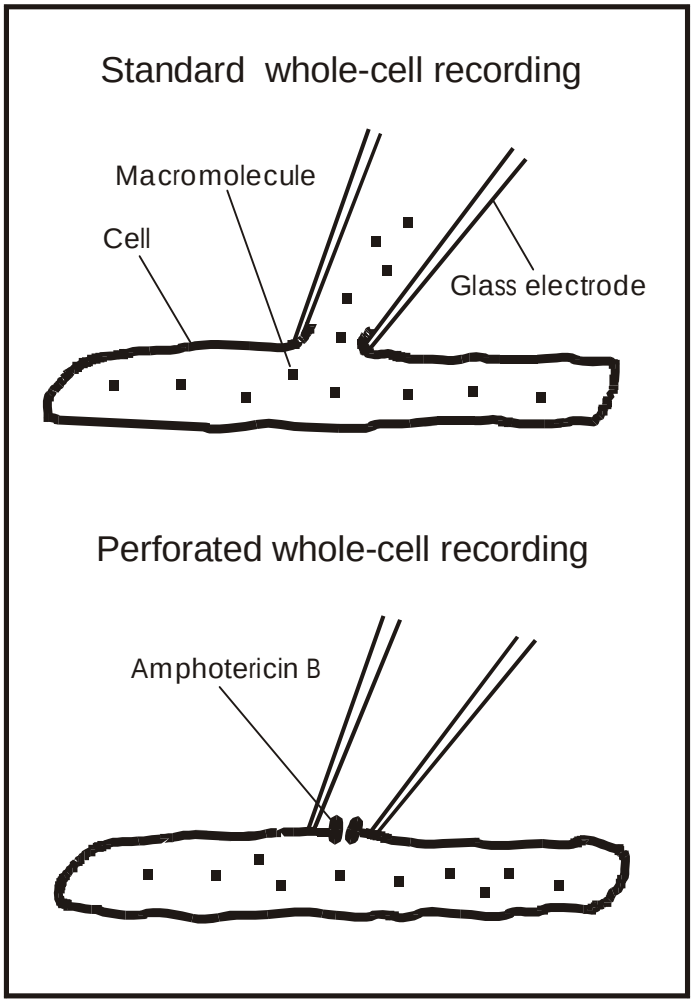

Figure 3. Two different types of the whole-cell patch-clamp configuration. In contrast to the standard configuration, the ampotericin B-perforated whole-cell patch-clamp configuration prevents the intracellular macromolecules from diffusing out of the cells.

The whole-cell voltage clamp was achieved by means of the EPC7 patch-clamp amplifier, connected via a 16 bit A/D interface to a Pentium IBM clone computer. The cell capacitance and series resistance were compensated before each measurement. The current and voltage signals were filtered at 3 kHz and subsequently sampled at 2 kHz. Data acquisition and analysis was performed with an ISO-3 multitasking patch-clamp program (MFK, Niedernhausen, Germany).

3.6 Action potential measurement in single cells

Action potentials of single ventricular myocytes were recorded using whole-cell current clamp. The composition of the electrode filling solution is shown in Table 2. The cells were stimulated by a current pulse of 4-ms duration and with an amplitude 10% above the threshold. Stimulation frequency was 0.5 Hz. The following parameters were evaluated: resting membrane potential, action potential amplitude, and action potential duration measured at 90% repolarization (APD_{90}). Only cells with a resting membrane potential more negative than -75 mV were used for the experiments.

3.7 Measurement of ionic currents

Whole-cell voltage clamp was used to measure the membrane ionic currents. In most cases, the recorded current amplitude was normalized by membrane capacitance (C_m) to obtain the current density. The value of C_m was calculated as the area under the uncompensated capacitative transient divided by the amplitude of a hyperpolarizing pulse of 5 mV (from -75 mV to -80 mV) applied immediately after formation of the whole-cell configuration. Depending on the type of currents being investigated, different electrode filling solutions were used. The composition of electrode filling solutions for the recording of various ionic currents is listed in Table 2.

3.7.1 L-type Ca^{2+} current

The L-type Ca^{2+} current ($I_{Ca(L)}$) was elicited in guinea-pig ventricular myocytes by applying a test pulse of 300-ms duration every 5 s from a holding potential of -80 mV. A prepulse to -40 mV of 40-ms duration preceded each test pulse to inactivate both fast Na^+ and T-type Ca^{2+} currents. Alternatively, the holding potential was set at -40 mV instead of -80 mV. The amplitude of $I_{Ca(L)}$ was measured as peak inward current with respect to the zero current level. To eliminate interfering K^+ currents, CsCl and Tetraethylammoniumchlorid (TEA-Cl) were included in the electrode filling solution (Table 2), and KCl in the Tyrode solution was replaced by equimolar CsCl.

3.7.2 Voltage-dependent K^+ currents

Steady-state membrane K^+ currents which include mainly the inward rectifier K^+ current (I_{K1}) and the delayed rectifier K^+ current (I_K) were elicited in guinea-pig ventricular myocytes by applying hyperpolarizing and depolarizing test pulses ranging from –100 to 40 mV for 1 s from a holding potential of -40 mV at a rate of 0.1 Hz. The steady-state membrane K^+ current

was measured as the net current at the end of the clamp step with respect to the zero current level. In order to measure the background currents activating in the potential range of –100 to 0 mV, test pulses of 100-ms duration were applied from a holding potential of –40 mV, and 1 mM $BaCl_2$ was included in the bath solution to block the interfering I_{K1}.

More reliable determination of I_K in guinea-pig ventricular myocytes was achieved by measuring the outward tail currents elicited on repolarization to -40 mV at the end of 1-s or 250-ms depolarizing clamp steps. The amplitude of the deactivating I_K tail was measured as the difference between the peak outward tail current and the steady-state current at -40 mV. In some experiments, nominally Ca^{2+}-free Tyrode solution was used to allow measurement of the rapidly activating I_K (I_{Kr}) without contamination of the slowly activating I_K (I_{Ks}) (Sanguinetti and Jurkiewicz, 1990b; Jurkiewicz and Sanguinetti, 1993). In this case, cells were depolarized to -10 mV for 500 ms from a holding potential of -40 mV. Both the steady-state current at the end of depolarization and the tail current upon repolarization were evaluated.

The transient outward current (I_{to}) was measured in rat ventricular myocytes by applying test pulses of 500 ms every 5 s from a holding potential of -80 mV. To inactivate interfering Na^+ currents, a prepulse of 100 ms to -60 mV preceded each test pulse.

For the measurement of all the aforementioned voltage-dependent K^+ currents or background currents, the external bath solution contained 0.3 µM nisoldipine in order to block interfering $I_{Ca(L)}$.

3.7.3 Muscarinic receptor gated K^+ current

Guinea-pig atrial myocytes were used for the measurement of muscarinic receptor gated K^+ currents ($I_{K,ACh}$). The membrane potential was clamped constantly at -50 mV. Since the K_{ACh} channels are directly activated by membrane delimited G_i-proteins (Yamada, et al., 1998), $I_{K,ACh}$ was induced either by superfusing the cells with 1 µM carbamylcholine or 1 µM (-)-N^6-phenylisopropyladenosine (R-PIA) to stimulate G_i-protein coupled muscarinic- or adenosine receptors, respectively, or by including 100 µM Guanosine-5'-O-(3-thiotriphosphate) (GTP-γS) in the electrode filling solution to persistently activate the G_i-proteins.

3.8 Cell shortening

Single ventricular myocytes were stimulated at 0.5 Hz by either current clamp or action potential clamp (AP clamp) in the whole-cell patch-clamp configuration. The composition of electrode filling solution was as same as that for single-cell action potential measurement

(Table 2). For AP clamp, action potentials were recorded from a typical cell in the current clamp mode and stored in the computer. These action potentials served then as voltage-commands to clamp other cells and to elicit contractions. Cell length was monitored using a stable light source (Gossen-Konstanter, Erlangen, Germany) to form a bright field image of the cell, which was projected onto a photodiode array (Laser 2000, Weßling, Germany) with a 4-ms scan rate, and changes in cell length during contraction were quantified via edge tracking. The signal was then transmitted to a computer for on-line analysis. Peak shortening, time to peak shortening, relaxation time and shortening duration (measured at 80% of relaxation) were evaluated.

3.9 Ca^{2+} transients

Guinea-pig ventricular myocytes were added to the recording chamber mounted on an inverted microscope adapted for epifluorescence measurement (Figure 4). Single cells were loaded for 5-10 min via the patch electrode filled with 30 µM of the Ca^{2+}-senstive dye fura-2 pentasodium salt dissolved in the electrode filling solution (for composition see Table 2). The dye was alternately (200 Hz) excited at 340- and 380-nm wavelengths of light generated by a Deltascan illumination system (Photon Technology International, Brunswick, NJ, U.S.A). Emission fluorescence at 510 nm was detected with a photon-counting photomultiplier tube (Model 810, Photon Technology International) and subsequently transferred to a computer. Data acquisition and analysis was carried out by a Felix^{TM} program (Photon Technology International). Autofluorescence of the cells was measured after establishment of a gigaohm-seal and was subsequently subtracted from the recorded data. Intracellular calibration procedure was adapted from a method described previously (Ganitkevich and Isenberg, 1991). The ratio (R) of fluorescence signals recorded at 340 and 380 nm excitation wavelengths was converted to intracellular Ca^{2+} concentration ($[Ca^{2+}]_i$) by the following equation:

$$[Ca^{2+}]_i = K_d \times [(R-R_{min})/(R_{max}-R)] \times Sf_{380}/Sb_{380}$$

where K_d is the dissociation constant of fura-2 which was taken as 224 nM (Grynkiewicz et al, 1985); R_{min} and R_{max} are the fluorescence ratio values under Ca^{2+}–free and Ca^{2+}–saturating conditions, respectively, and Sf_{380} and Sb_{380} are the fluorescence values for Ca^{2+}–free and Ca^{2+}–saturating forms of fura-2 measured at 380 nm excitation wavelength. R_{max} and Sb_{380} were determined by superfusing the cells with bath solution containing 2 mM Ca^{2+} and 10 µM of the Ca^{2+}-ionophore ionomycin, and by voltage-clamping the membrane potential to –200

mV. To obtain the values of R_{min} and Sf_{380}, cells were perfused with an electrode filling solution containing 10 mM EGTA.

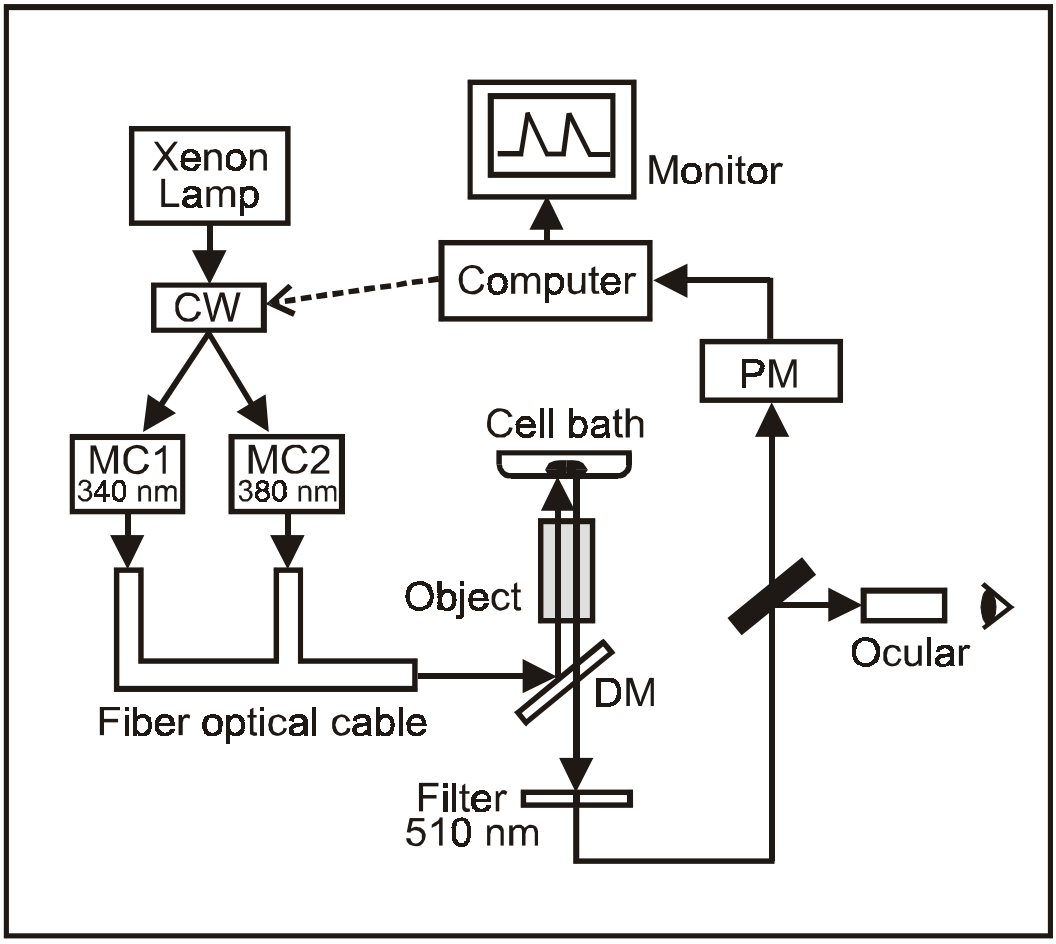

Figure 4. Schematic drawing of the experimental setup for the measurement of the intracellular Ca^{2+} transient using fura-2 fluorescent indicator. Excitation light coming from xenon lamp is directed alternatively via a automatically controlled chopper wheel (CW) to two monochromators (MC1 or MC2) which are set at 340 or 380 nm wavelength, respectively. The monochromatic light from MC1 or MC2 is then directed via a fiber optical cable onto a dichroic mirror (DM) which on the one side reflects the monochromatic light to the fura-2 loaded single cell, and on the other side permits the fluorescent light emitted from the cell to pass through. After being filtered by a 510 nm filter, the emission light is detected by a photomultiplier (PM) which then transferred the converted signals to a computer for on-line analysis.

3.10 Membrane preparation

Sarcolemmal membranes were prepared from frozen left atrial tissues from a patient with dilated cardiomyopathy who underwent cardiac transplantation. The tissues were minced with scissors and homogenized in 8-fold volumes of ice-cold homogenization buffer (50 mM Tris, 5 mM $MgCl_2$, 5 mM EDTA, 1 mM EGTA, and 2 µg/ml aprotinin, pH adjusted to 7.5) with an

Ultraturrax homogenizer three times for 15 sec at maximal speed. The homogenate was filtered through a 200-µm gauze and centrifuged for 30 min at 4 °C and 500 × g. The supernatant was supplemented with 107 mM KCl and 20 mM MOPS, pH 7.4; incubated for 10 min on ice; and centrifuged for 60 min at 100,000 × g at 4 °C. The pellet was resuspended in 60 mM KCl and 20 mM Tris, pH 7.4, with a short burst of an Ultraturrax at medium speed and respun at 100,000 × g for 45 min at 4 °C. The final pellet was resuspended in homogenization buffer and stored in aliquots at -80 °C. The protein yield was 9.92 mg/g wet weight as determined according to Bradford (1976) using bovine serum albumin as a standard.

3.11 Radioligand binding

The density of the muscarinic receptors was determined by saturation binding experiments with the nonselective muscarinic receptor antagonist [^{3}H]-quinuclidinyl benzylate ([^{3}H]-QNB, 42 Ci/mmol) at room temperature (22-24°C), using 40-80 µg membrane protein in an assay buffer of 20 mM Tris, 100 mM NaCl, 0.5 mM EDTA, pH 7.4, and in total volume of 250 µl. The reaction was terminated by rapid filtration through glass-fiber filters (MAFB NOB; Millipore, Bedford, U.S.A.). The radioactivity bound to the filters was determined by scintillation counting after an over-night incubation. Association/dissociation kinetics were tested over 120 min of association and 120 min of dissociation after the addition of 1 µM atropine at 90 min. Under these conditions, binding reached an equilibrium after 60 min and remained stable between 60 and 120 min. All further reactions were performed after a 90-min incubation in triplicate. Non-specific binding was defined as bound radioligand in the presence of 1 µM atropine and was subtracted from the total binding to calculate specific binding. To test whether MTO competes with [^{3}H]-QNB for binding to human atrial membranes, two sets of experiments were performed. First, saturation experiments with [^{3}H]-QNB were performed in the absence and presence of 30 µM MTO. Second, binding of several fixed concentrations of [^{3}H]-QNB (0.70 to 2.91 nM) was displaced by MTO (0.1 to 1000 µM). All reactions were performed at least twice in triplicate. The software GraphPad (San Diago, U.S.A.) was used to fit displacement curves and to calculate dissociation constants.

3.12 Chemicals

- Amphotericin B: Sigma-Aldrich Chemie GmbH, Deisenhofen, Germany

- Atropine: Sigma-Aldrich Chemie GmbH, Deisenhofen, Germany
- Carbamylcholine: Sigma-Aldrich Chemie GmbH, Deisenhofen, Germany
- D-Sotalol: Bristol-Myers Co., Wallingford, CT, U.S.A.
- Fura-2 pentasodium salt: Calbiochem-Novabiochem Co., La Jolla, CA, U.S.A.
- Guanosine-5'-O-(3-thiotriphosphate): Sigma-Aldrich Chemie GmbH, Deisenhofen,Germany
- [^{3}H]-quinuclidinyl benzylate: DuPont-New England Nuclear, Boston, U.S.A.
- (±)-Isoproterenol: Sigma-Aldrich Chemie GmbH, Deisenhofen, Germany
- Mitoxantrone hydrochloride: Lederle GmbH, Münster, Germany
- Nisoldipine: Bayer AG, Wuppertal, Germany
- (-)-N^6-phenylisopropyladenosine: Sigma-Aldrich Chemie GmbH, Deisenhofen, Germany
- Tetrodotoxin: Sigma-Aldrich Chemie GmbH, Deisenhofen, Germany

3.13 Statistics

Where appropriate, results are presented as means ± SEM. Significance tests were performed using Student's *t* test for paired observations. Differences between means were regarded statistically significant at $p < 0.05$.

4. Results

4.1 Action potential duration in papillary muscles

As shown in Figure 5A and substantiated in four other papillary muscles, 30 µM MTO produced a time-dependent prolongation of APD at all levels of repolarization. Three hours after the application of MTO, APD measured at 90% repolarization (APD_{90}) had increased from 223 ± 14 ms (control) to 295 ± 18 ms, i.e. by 32% (Figure 5B, n = 5). MTO had no significant effects on resting membrane potential, V_{max}, and action potential amplitude. The values before (n = 5) and 3 h after the addition of 30 µM MTO were –84 ± 1 and –85 ± 2 mV

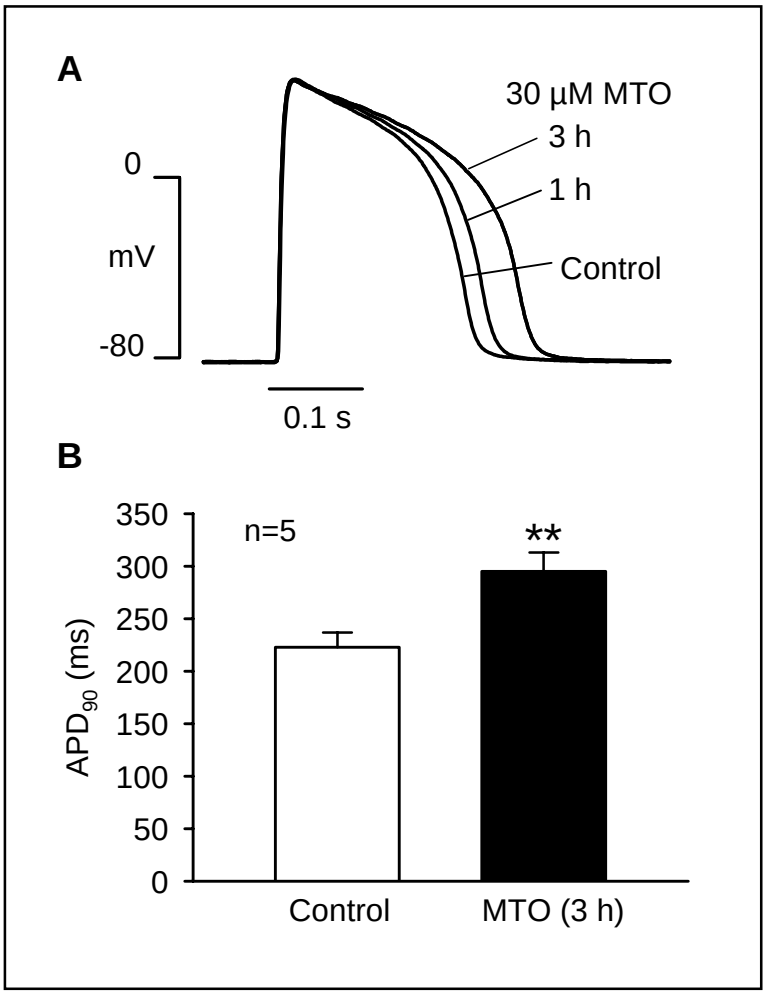

Figure 5. Prolongation of action potential duration (APD) induced by MTO in guinea-pig ventricular papillary muscles. The muscles were electrically stimulated at 0.5 Hz. A, superimposed original recordings showing the time-dependent prolongation of APD in the presence of 30 µM MTO. B, summary of the increase in APD measured at 90% repolarization (APD_{90}) 3 h after incubation with 30 µM MTO. **, $p<0.01$ versus control.

for the resting potential, 214 ± 19 and 203 ± 16 V/s for V_{max}, and 120 ± 4 and 118 ± 3 mV for the action potential amplitude.

Figure 6 shows that APD prolongation induced by 30 µM MTO was successively reduced by increasing the stimulation frequency. As shown by the original action potentials in Figure 6A, MTO completely lost its APD-prolonging effect at a stimulation frequency of 4 Hz. Figure 6B compares the influence of stimulation frequency on the extent of APD prolongation induced

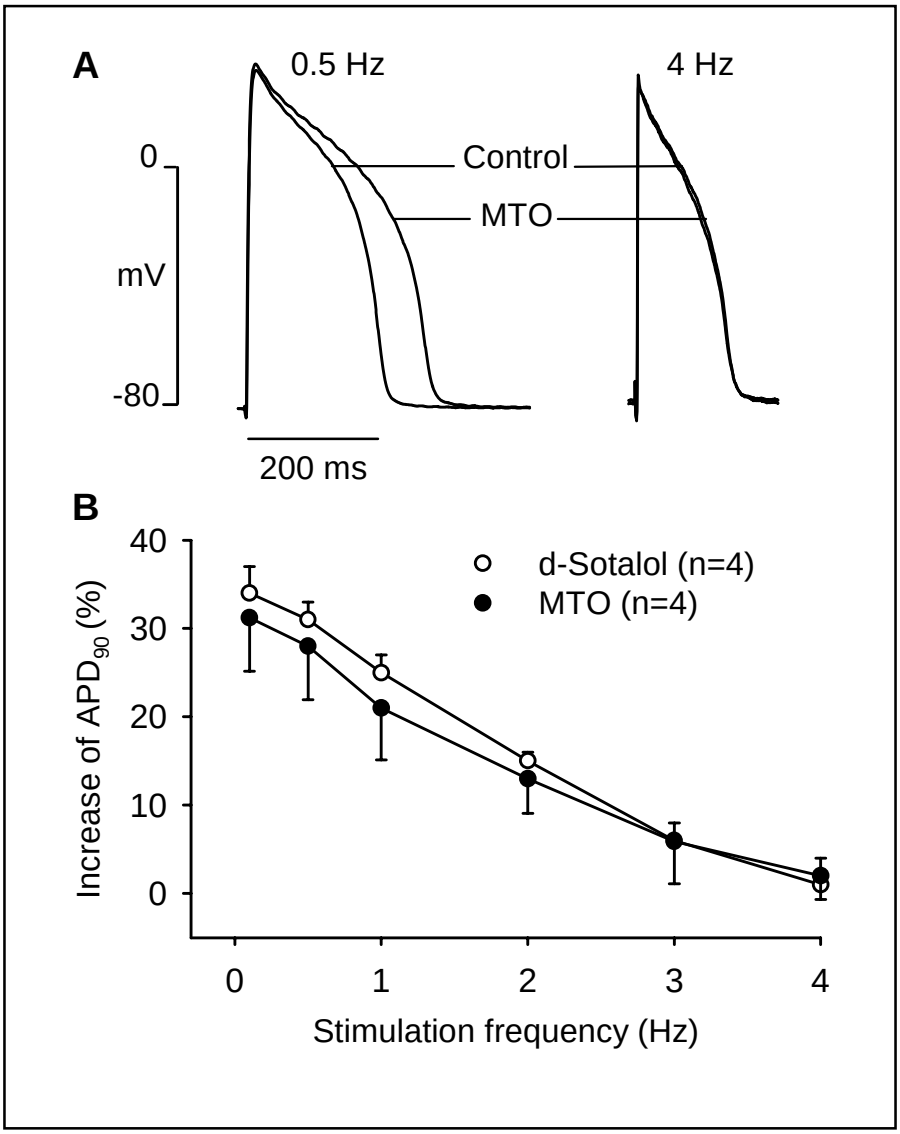

Figure 6. Reverse rate-dependence of the prolongation of action potential duration (APD) by MTO in guinea-pig ventricular papillary muscles. The effect of MTO was measured 3 h after its addition to the bath. A, superimposed original recordings showing the effect of 30 µM MTO on APD in the same muscle at two different stimulation frequencies. B, comparison of the reverse rate-dependence of the prolongation of APD_{90} by 30 µM MTO and 30 µM d-sotalol. The effect of d-sotalol was evaluated 30 min after its addition to the bath. Two different groups are compared.

by 30 µM MTO and 30 µM d-sotalol, a class III antiarrhythmic drug. It can be clearly seen that APD prolongation caused by both drugs exhibit reverse rate-dependency.

4.2 Action potential duration in ventricular myocytes

The effect of MTO on action potential duration (APD) was also investigated in isolated guinea-pig ventricular myocytes that had been current-clamped in the whole-cell clamp configuration (Figure 7). In the absence of MTO, cells stimulated at 0.5 Hz had resting potentials in the range -76 to -85 mV (mean of thirteen cells -79.3 ± 0.7 mV) and displayed action potentials with a mean duration of 260.7 ± 7.7 ms when measured at 90% repolarization (n = 13). As shown in Figure 7B, without drug-intervention APD_{90} shortened

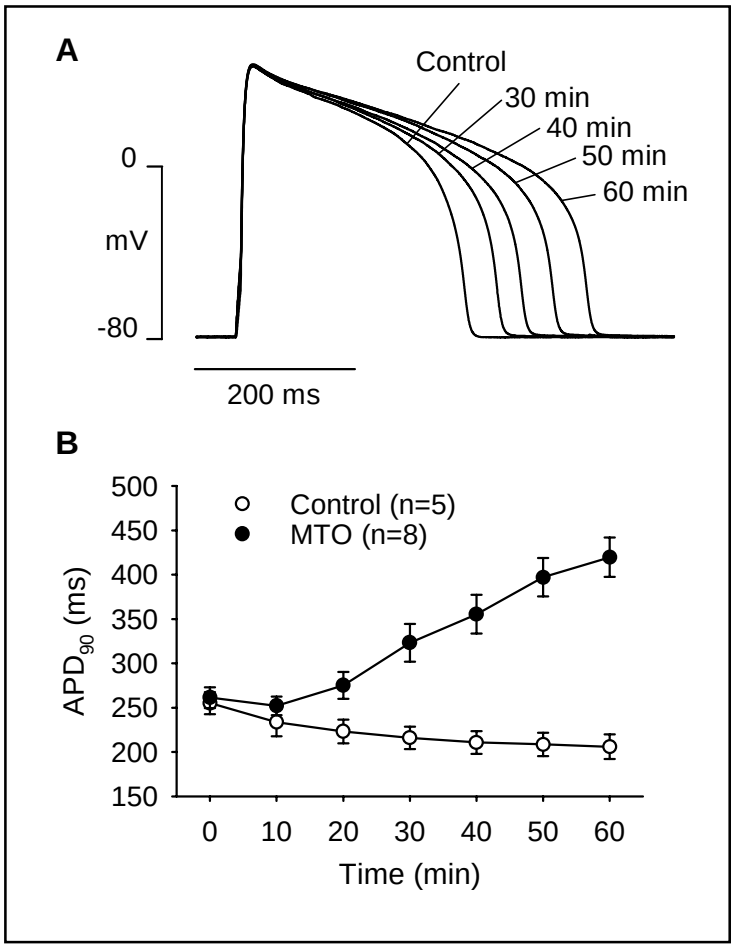

Figure 7. Effect of MTO on the action potential duration (APD) in guinea-pig ventricular myocytes. Action potentials were evoked with current-clamp at a frequency of 0.5 Hz. A, recordings showing time-dependent prolongation of APD induced by 30 µM MTO. All action potentials were continuously recorded from one cell. B, time-dependent change of APD_{90} in control cells and in cells superfused with 30 µM MTO.

under continuous stimulation within 1 h by 19.3% (n = 5), whereas MTO prolonged APD_{90} after 1 h by 60.6% (n = 8). Not surprisingly for cells with such a pronounced prolongation of APD, some cells exposed for more than 1 h to 30 µM MTO displayed early after-depolarizations (Figure 8).

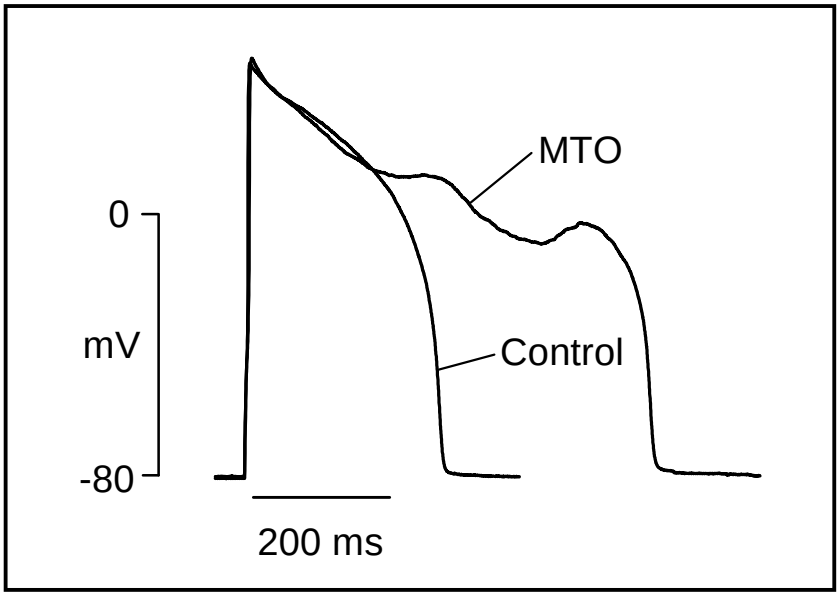

Figure 8. Superimposed original traces showing the early afterdepolarization recorded from a guinea-pig ventricular myocyte which had been treated with 30 µM MTO for 1 h. The cell was stimulated at 0.5 Hz under current clamp.

In three other cell groups, APD_{90} was determined after 1 h of incubation with either 30 µM MTO, 10 µM tetrodotoxin (TTX), or 10 µM TTX plus 30 µM MTO. As shown in Figure 9, APD_{90} of six cells treated with 30 µM MTO was 500.5 ± 36.5 ms and thus significantly longer than APD in untreated cells ($P<0.01$). The ability of MTO to prolong APD was preserved in the presence of TTX. Although TTX significantly shortened APD_{90} as has previously been observed (Kiyosue and Arita, 1989), MTO prolonged APD_{90} in the presence of TTX to 463.2 ± 22.9 ms (n = 8; Figure 9). There was no significant difference in the prolongation of APD by MTO when TTX was present; MTO increased APD_{90} by 91.8% in the absence and by 100.4 % in the presence of 10 µM TTX. The results clearly exclude the possibility of a TTX-sensitive Na^+ window current contributing to the APD prolongation produced by MTO. Other parameters of the action potential, such as resting potential and action potential amplitude, were not significantly affected by MTO.

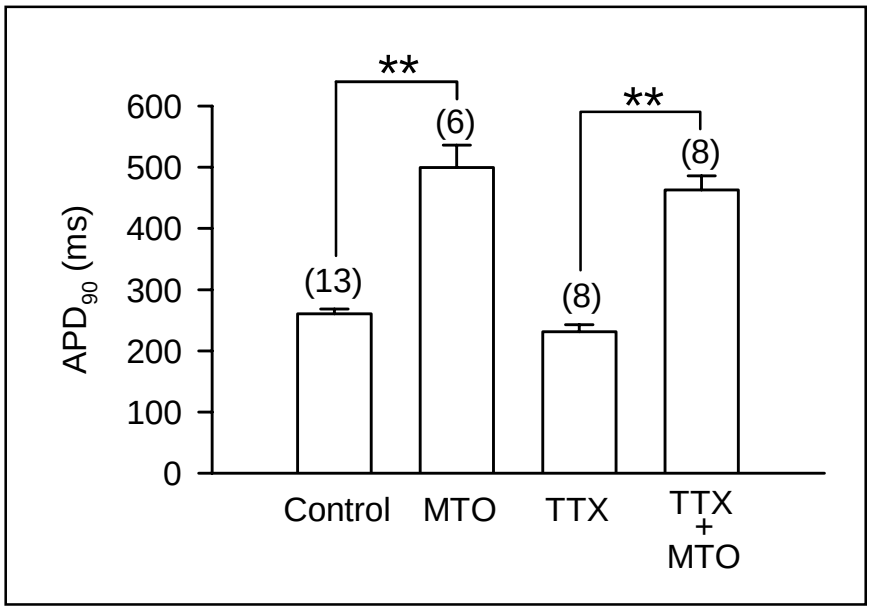

Figure 9. Failure of tetrodotoxin (TTX) to prevent the prolongation of APD_{90} induced by superfusion of guinea-pig ventricular myocytes with 30 µM MTO for 1 h. The cells were stimulated at 0.5 Hz under current clamp. APD_{90} was measured in the absence (Control) and in the presence of either 30 µM MTO, 10 µM TTX, or 30 µM MTO plus 10 µM TTX. Data from four different cell groups are compared. Numbers of cells in each group are given in parentheses. **, $p<0.01$.

4.3 Voltage-dependent K^+ currents

To test for a possible interaction of MTO with K^+ currents, myocytes were clamped from a holding potential of -40 mV to voltages between -100 and +40 mV in 10-mV steps for 1 s. As shown by the current-voltage relations in Figure 10, pretreatment of cells with 30 µM MTO for 1 h produced a significant decrease of the inward rectifier K^+ current (I_{K1}). K^+ currents activated at potentials positive to -30 mV, i.e., potentials at which the time-dependent delayed rectifier K^+ current (I_K) activates, were likewise suppressed by 30 µM MTO. Currents elicited by clamp steps to voltages positive to +20 mV, however, were not inhibited by MTO. The effect of MTO on I_K was therefore investigated in more detail by measuring the outward tail currents elicited on repolarization to -40 mV after depolarizing step potentials from a holding potential of -40 mV to +70 mV in 10 mV increments for 1 s. Typical recordings obtained

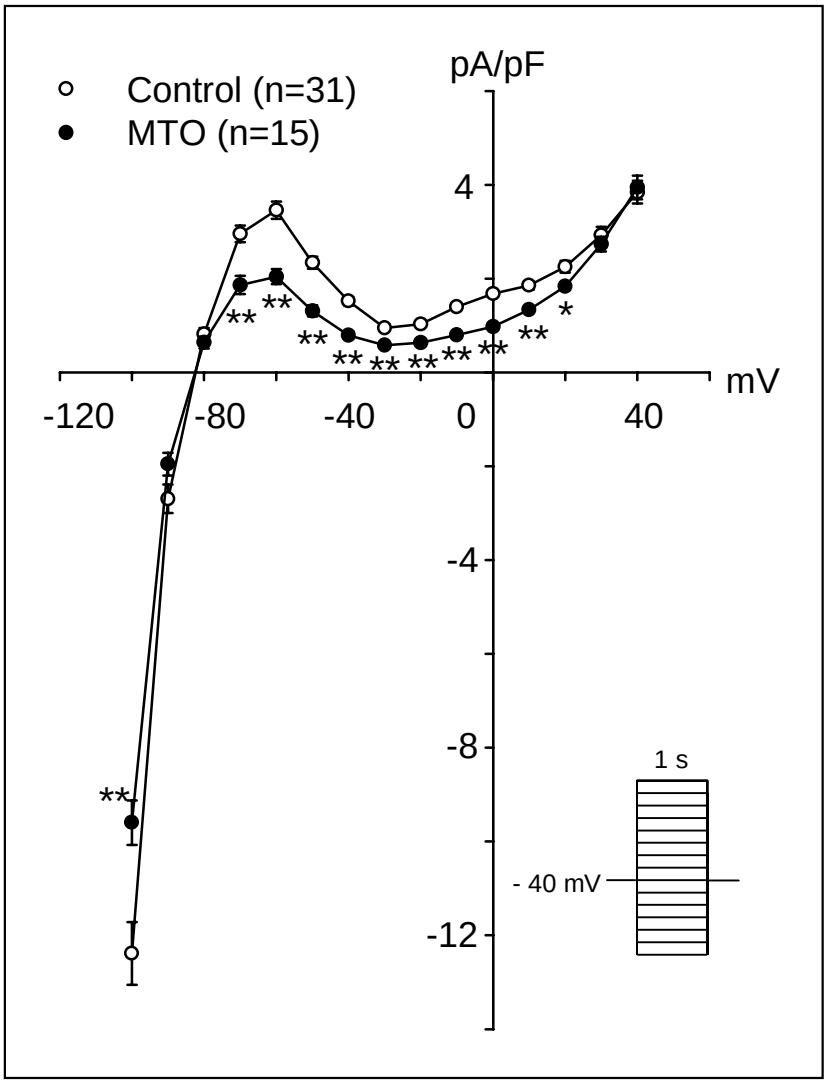

Figure 10. Current-voltage relation of the steady-state K^+ currents of guinea-pig ventricular myocytes in the absence (Control) and in the presence of 30 µM MTO. The drug effect was measured 1 h after its addition to the cells. Currents were evoked by applying 1-s depolarizing or hyperpolarizing pulses in 10 mV steps from a holding potential of -40 mV every 10 s as depicted in inset. The mean current densities are plotted against the respective test potentials. Data from two different cell groups are compared. *, $p<0.05$ and **, $p<0.01$ versus control.

from two different cells clamped from -40 to +60 mV in several steps are shown in Figure 11A; peak tail currents are clearly suppressed at all potentials in the MTO-pretreated cells whereas time-dependent I_K was not affected at potentials positive to +20 mV. In Figure 11B, tail currents were plotted as a function of membrane potential, and it can be seen that currents in the presence of MTO (closed circles) were suppressed at all voltages. Inspection of Figure 11B reveals that the current-voltage relations in the absence and in the

presence of MTO are characterized by an outward hump which indicates that I_K is composed of a low (-30 to +10 mV) and a high voltage (>+20 mV) component.

Figure 12 (open circles) demonstrates that inhibition of I_K tail currents by MTO is largest at lower voltages (by 50 to 60% at -30 to +10 mV) and decreases at more positive potentials. When I_K tail currents were elicited by short voltage pulses of 250 ms, inhibition by MTO did not differ from long pulses in the lower voltage range but was more sustained at more positive potentials (Figure 12, closed circles).

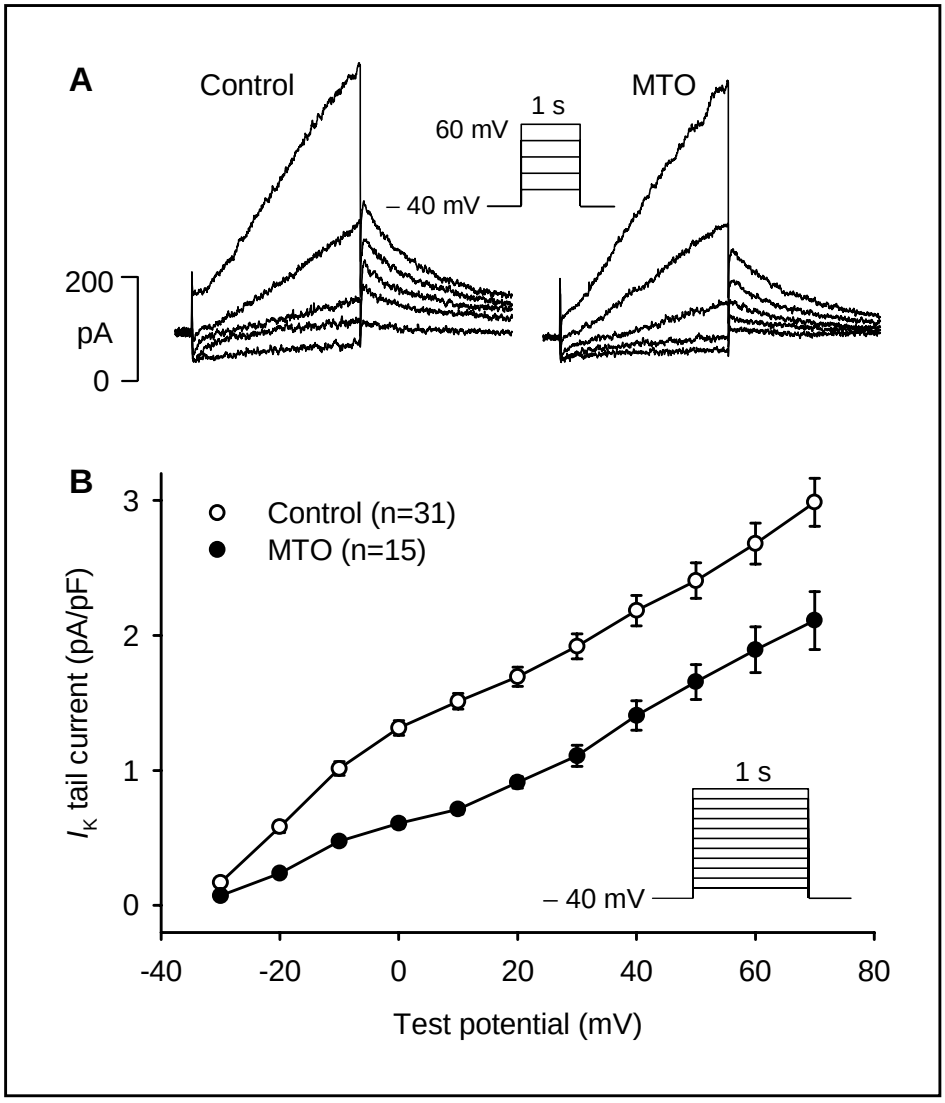

Figure 11. Inhibition of I_K by MTO in guinea-pig ventricular myocytes. I_K was elicited very 10 s by voltage protocols as indicated in the inset of panel A and B. The drug effect was determined 60 min after its addition to the myocytes. A, superimposed traces showing I_K steady-state currents and tail currents of a control cell (C_m=80 pF) and of a cell superfused with 30 µM MTO (C_m=83 pF). B, I_K tail current-voltage relations in the absence (control) and in the presence of 30 µM MTO. The mean I_K tail current densities from two different cell groups at the respective test potentials are compared.

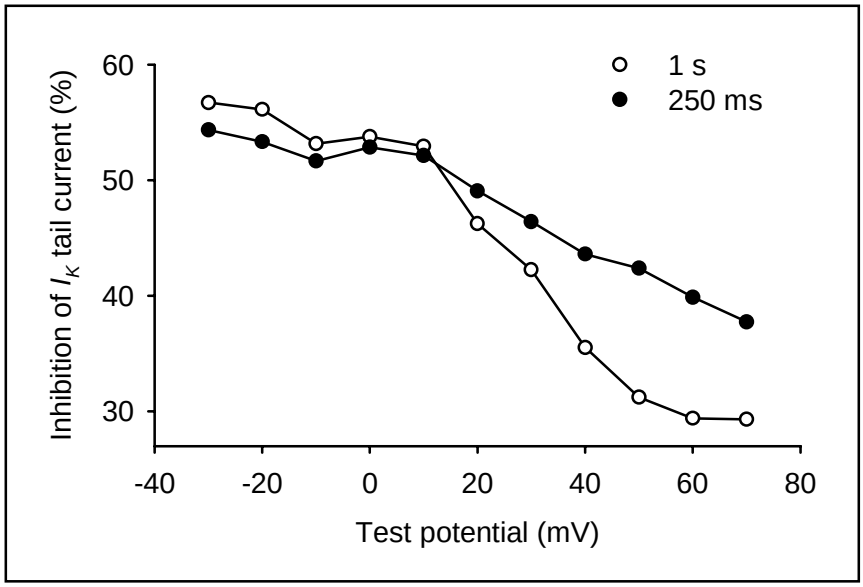

Figure 12. Effect of test pulse duration on the voltage-dependent inhibition of I_K tail currents by 30 μM MTO. Guinea-pig ventricular myocytes were clamped every 10 s from a holding potential of -40 mV to test potentials up to +70 mV in 10 mV increments. Test pulses of 1-s and 250-ms were applied to every cells. Percent inhibition of the I_K tail current was calculated by dividing the mean current densities of the cells pretreated with 30 μM MTO for 1 h (n=15) by that of control cells (n=31) at the respective test potential and test pulse duration.

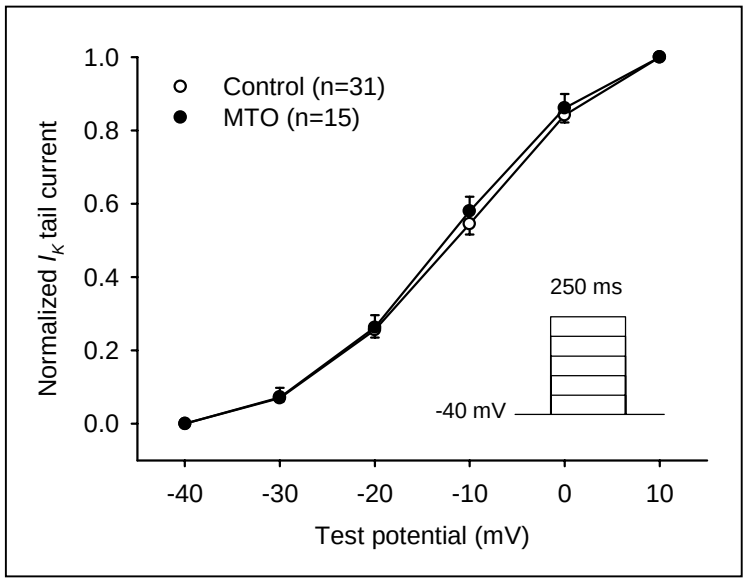

Figure 13. Lack of voltage dependence of the action of MTO on the I_K component covering the lower voltage range. Guinea-pig ventricular myocytes were clamped every 10 s from a holding potential of –40 mV to test potentials ranging from -30 mV to 10 mV in 10 mV increments for 250 ms. The measured peak I_K tail currents in the absence (Control) and in the presence of 30 μM MTO were normalized to that elicited after depolarizing step to 10 mV.

In Figure 13, tail currents obtained with 250 ms pulses were normalized relative to the respective tail current amplitude elicited at +10 mV. It can be seen that both curves are superimposable, which excludes a voltage dependence of the action of MTO on the I_K component covering the lower voltage range. These results suggested that MTO preferentially inhibited the rapid activating component of I_K (I_{Kr}). When I_{Kr} was measured directly in cells bathed in nominally Ca^{2+}-free solution, both the steady-state current evoked by a 500-ms depolarizing step to -10 mV and the tail current elicited upon depolarization to a holding potential of -40 mV were significantly inhibited by 64% after 1 h treatment with 30 µM MTO (Figure 14).

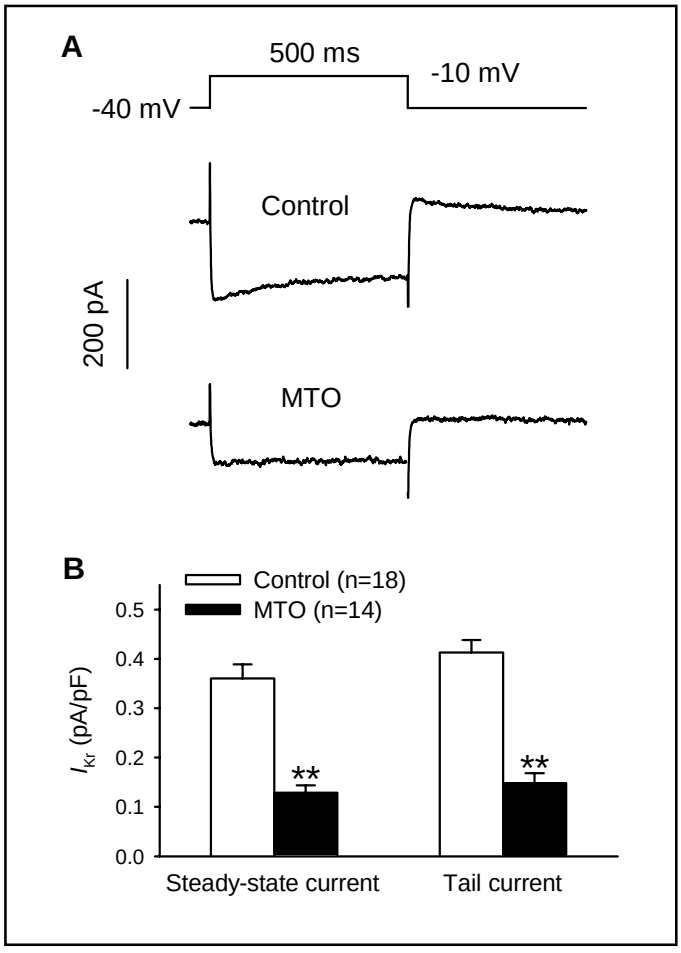

Figure 14. Inhibition of I_{Kr} by 30 µM MTO. Guinea-pig ventricular myocytes were superfused with nominally Ca^{2+}-free bath solution. I_{Kr} steady-state current was evoked by a 500-ms depolarizing pulse to -10 mV at 0.5 Hz, and I_{Kr} tail current was elicited upon repolarization to a holding potential of -40 mV. The effect of MTO was measured after cells had been treated with the drug for 1 h. A, original current traces recorded from a control cell as well as a MTO-treated cell. Voltage protocol is shown in the top panel. B, the mean current densities of the I_{Kr} steady-state current as well as the tail current are compared between control cells and MTO-treated cells. **, $p<0.01$.

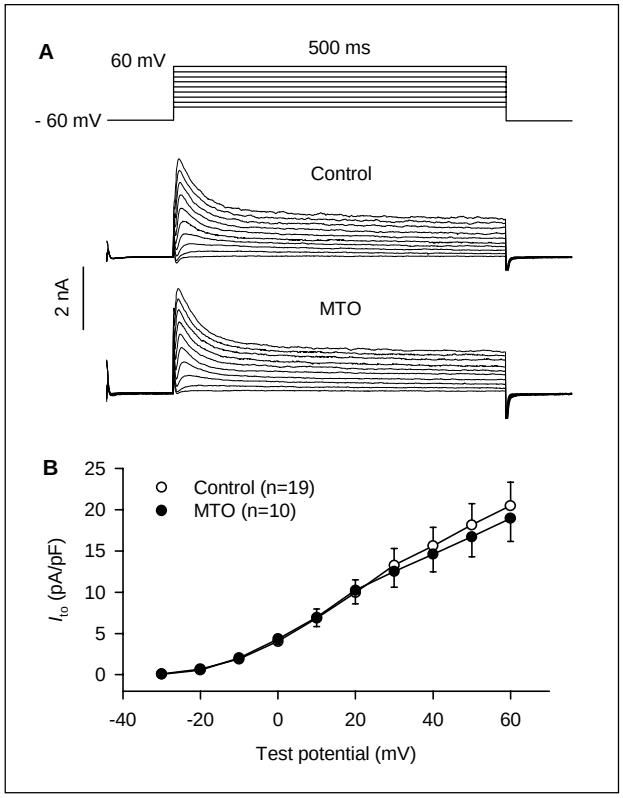

Figure 15. Failure of 30 mM MTO to influence I_{to} of rat ventricular myocytes. I_{to} was elicited by depolarization to various test potentials for 500 ms after a 100 ms prepulse to -60 mV from a holding potential of -80 mV every 10 s. A, superimposed original recordings showing representative I_{to} of a control cell (C_m= 135 pF) and of a MTO-treated cell (C_m= 129 pF). Top panel depicts voltage protocol used for the experiments. B, comparison of current-voltage relation of I_{to} in control cells and in cells pretreated with 30 µM MTO for 1 h.

Figure 16. A, superimposed original traces showing the time-dependent effect of 30 µM MTO on the action potential of a rat ventricular myocyte. The cell was current-clamped at 0.5 Hz. B, inhibition of I_{K1} by 30 µM MTO in rat ventricular myocytes. The currents were elicited by 1-s hyperpolarizing or depolarizing pulses in 10 mV steps from a holding potential of –40 mV every 10 s. The mean current densities are plotted against the respective test potentials. Data from two different cell groups are compared.

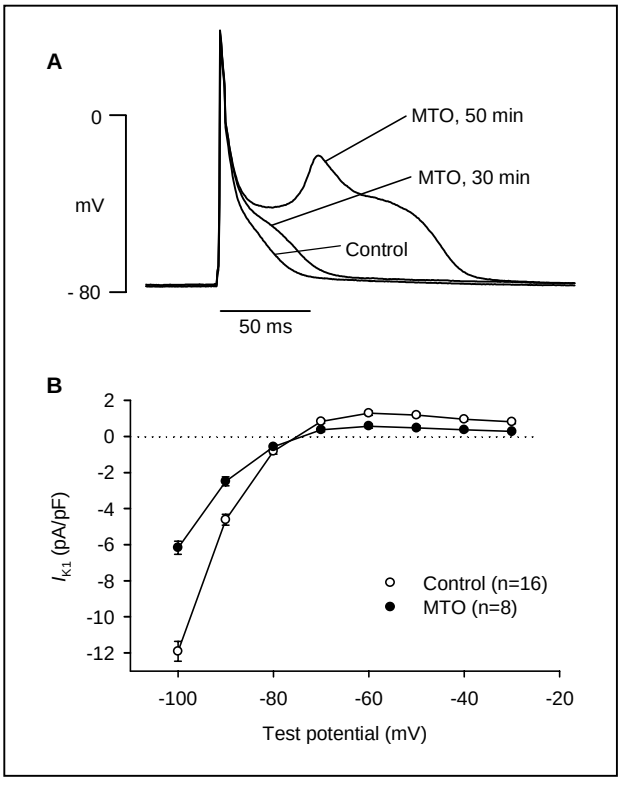

In some tissues such as rat and human heart, the transient outward K^+ current, I_{to}, also plays an important role in determining APD. Because I_{to} is functionally absent in guinea-pig ventricular myocytes (Josephson *et al*., 1984), experiments were also carried out on isolated rat cardiomyocytes. Cells were depolarized from a holding potential of -80 mV by a prepulse to -60 mV and than clamped to test potentials ranging from -30 to +60 mV for 500 ms. As shown by the original recordings in Figure 15A, and verified in additional 19 control cells and 10 cells pretreated with 30 µM MTO for 1 hour (Figure 15B), no significant effect on I_{to} at any of the test potentials could be detected by the drug. The lack of MTO to affect I_{to} is also demonstrated by continuous AP measurements in current-clamped rat ventricular myocytes as shown in Figure 16A. In the voltage range where I_{to} is dominant, no influence on AP repolarization can be detected. However, when I_{K1} becomes activated at around -30 mV, MTO produced a time-dependent slowing of repolarization which eventually led to early afterdepolarizations. As shown before in guinea-pig cells, MTO also inhibited I_{K1} of rat cardiomyocytes (Figure 16B) and this effect can explain the pronounced prolongation of the late phase of the AP in the rat.

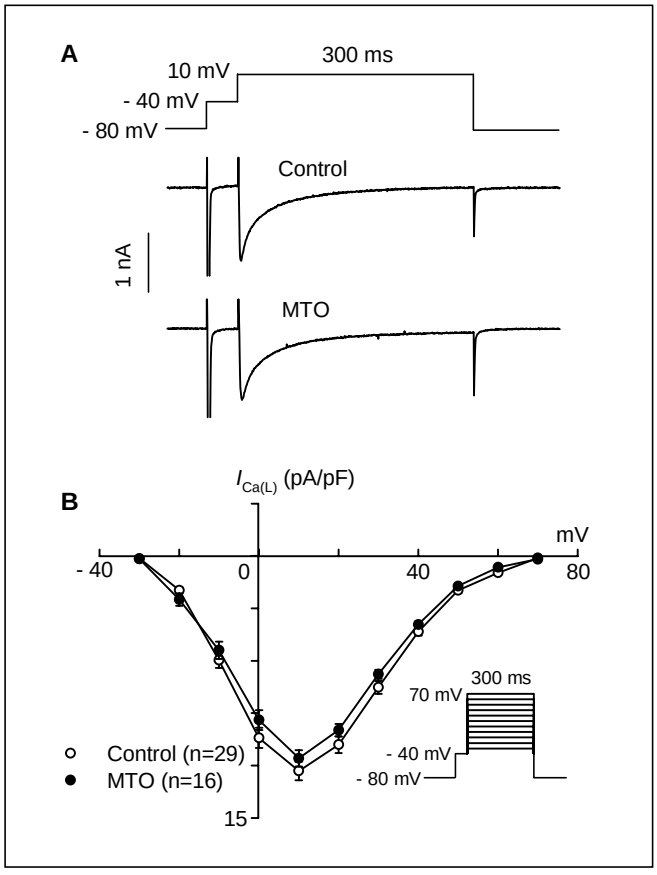

Figure 17. No effect of MTO on $I_{Ca(L)}$ in guinea-pig ventricular myocytes. The $I_{Ca(L)}$ was elicited by applying test pulses of 300-ms duration every 5s after a 40-ms prepulse to –40 mV from a holding potential of –80 mV. A, original recordings showing $I_{Ca(L)}$ of a control cell (C_m=102 pF) and of a cell treated with MTO for 1 h (C_m=99 pF). Voltage protocol is depicted in top panel. B, comparison of current-voltage relation of $I_{Ca(L)}$ in control cells and in cells treated with MTO for 1 h. Voltage protocols are shown in inset.

4.4 L-type Ca^{2+} current

When the L-type Ca^{2+} current, $I_{Ca(L)}$, was measured at various potentials in guinea-pig ventricular myocytes either in the absence or in the presence of 30 µM MTO, no significant difference in the peak amplitude or the inactivation kinetics of the current was observed (Figure 17). In the experiment shown in Figures 18A and B, $I_{Ca(L)}$ was enhanced from 0.7 to 2.0 nA by superfusing the myocyte with 50 nM isoproterenol. The isoproterenol-stimulated $I_{Ca(L)}$ was then inhibited by 1 µM carbamylcholine (CCh) to 1.3 nA. Adding 30 µM MTO to the isoproterenol- and CCh containing bath solution partially reversed $I_{Ca(L)}$ to 1.9 nA. After

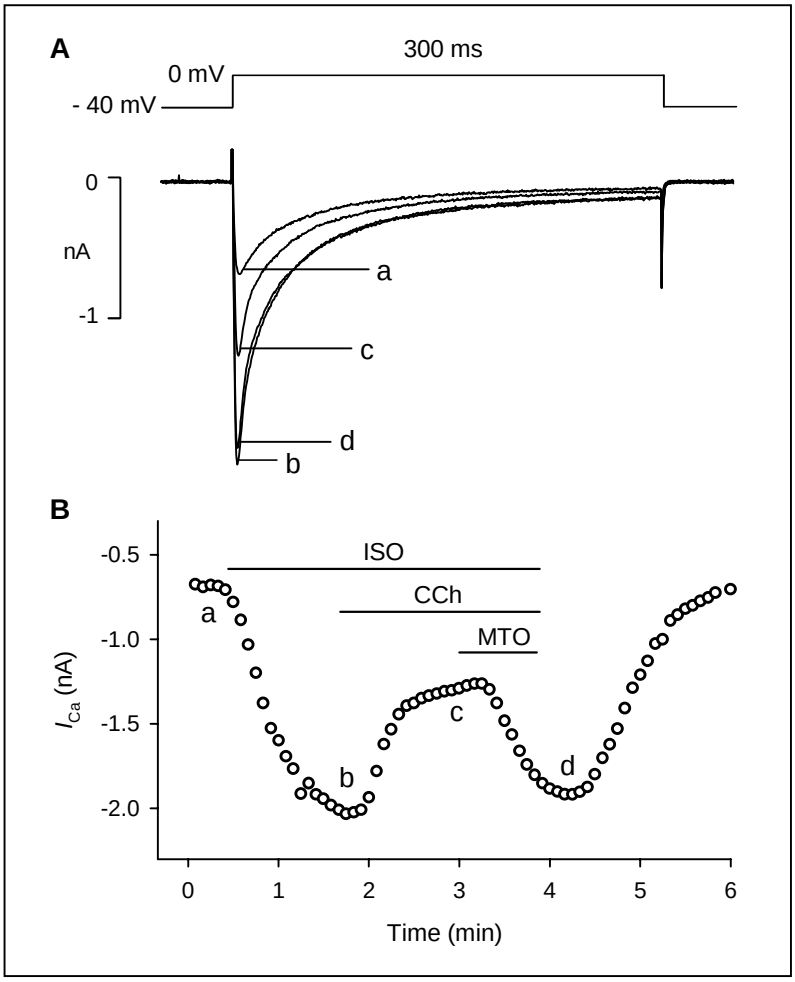

Figure 18. Reversal by MTO of the inhibitory effect of carbamylcholine on $I_{Ca(L)}$ activated by isoproterenol in guinea-pig ventricular myocytes. $I_{Ca(L)}$ was elicited by depolarizing steps from a holding potential of -40 mV to 0 mV for 300 ms at a frequency of 0.2 Hz. A, superimposed original current recordings from a typical cell showing the reversing effect of MTO on peak $I_{Ca(L)}$ inhibited by CCh. The current traces were recorded at the times indicated by the corresponding letters in panel B. The top panel shows voltage protocol used in the experiment. B, time course of the change of peak I_{Ca} in the same cell as in A. MTO, 30 µM mitoxantrone; ISO, 50 nM isoproterenol; CCh, 1 µM carbamylcholine.

washing out all three drugs, $I_{Ca(L)}$ returned to the predrug control level. In Figure 18A, the original current traces of the experiment depicted in Figure 18B are superimposed at times when the respective effects were maximal. Results similar to those shown in Figures 18A and B were obtained in eleven other cells (Figure 19A). In order to investigate whether MTO antagonized the effect of carbamylcholine by blocking muscarinic receptors or by interfering with mechanisms downstream to receptor activation, experiments with the A_1-adenosine receptor agonist (-)-N^6-phenylisopropyladenosine (R-PIA) were carried out. As shown in Figure 19B, addition of 1 µM R-PIA to myocytes stimulated by 50 nM isoproterenol induced a significant decrease of $I_{Ca(L)}$ from 2.2 ± 0.2 (ISO; n = 7) to 1.4 ± 0.2 nA (ISO + PIA). Contrary to CCh, the enhancing effect of additional MTO on $I_{Ca(L)}$ was not observed in the presence of isoproterenol and R-PIA (Figure 19B, ISO + PIA + MTO). These findings indicate that MTO enhanced $I_{Ca(L)}$ most likely by blocking muscarinic receptors.

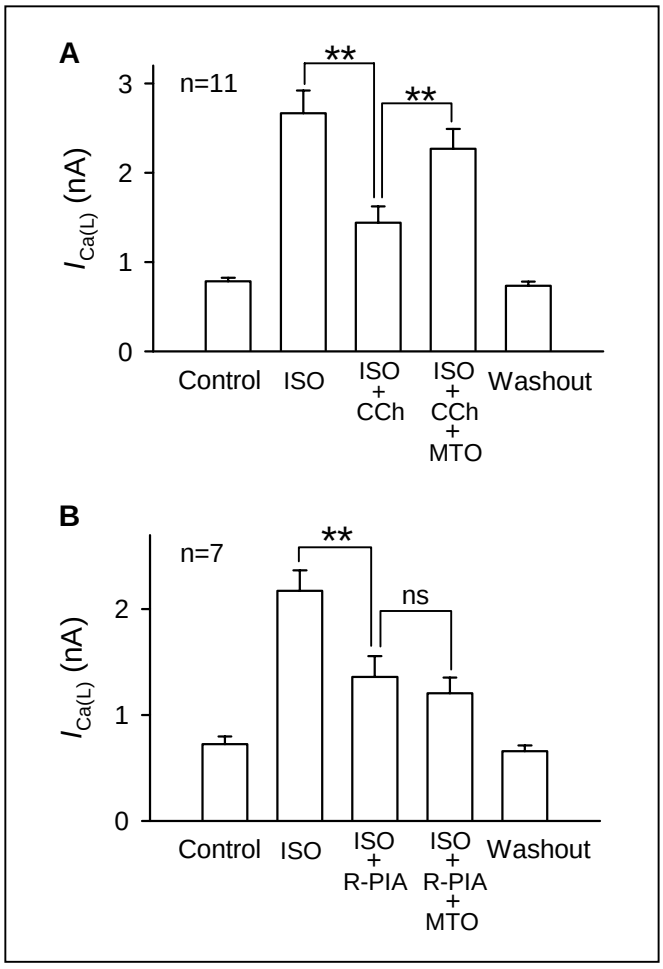

Figure 19. MTO selectively antagonizes the inhibitory effect of carbamylcholine but not that of R-PIA on $I_{Ca(L)}$ activated by isoproterenol in guinea-pig ventricular myocytes. The voltage protocol used to elicit $I_{Ca(L)}$ was the same as that illustrated in figure 18. MTO: 30 µM mitoxantrone; ISO: 50 nM isoproterenol; CCh: 1 µM carbamylcholine; R-PIA: 1 µM (-)-N^6-(2-phenylisopropyl)-adenosine. A, reversal by MTO of the inhibitory effect of CCh on peak $I_{Ca(L)}$. B, failure of MTO to antagonize the inhibitory effect of R-PIA on peak $I_{Ca(L)}$. **, p<0.01; ns, not significant.

4.5 Muscarinic receptor gated K^+ current

Cardiac muscarinic receptor gated K^+ channels (K_{ACh} channels) are present in high density in the atria, SA- and AV node, and are a major target of the vagal autonomic system in the heart. The effect of MTO on the CCh-induced K^+ current, i.e., $I_{K,ACh}$, in GTP (100 µM)-loaded guinea-pig atrial cells was therefore investigated. When 1 µM CCh was added to the superfusion medium, an outward K^+ current was rapidly activated at a holding potential of -50 mV (Figure 20A). After activation, the current slowly declined, possibly due to desensitization (Kurachi *et al*., 1987). Addition of 30 µM MTO after 1 min of CCh superfusion induced within a few seconds a marked depression of $I_{K,ACh}$ (Figure 20A). In eight cells, 1 µM CCh evoked an $I_{K,ACh}$ which amounted after 1 min to 188.3 ± 35.0 pA and was markedly depressed to 13.3 ± 3.5 pA, i.e. by 93%, when 30 µM MTO was added (Figure 20B).

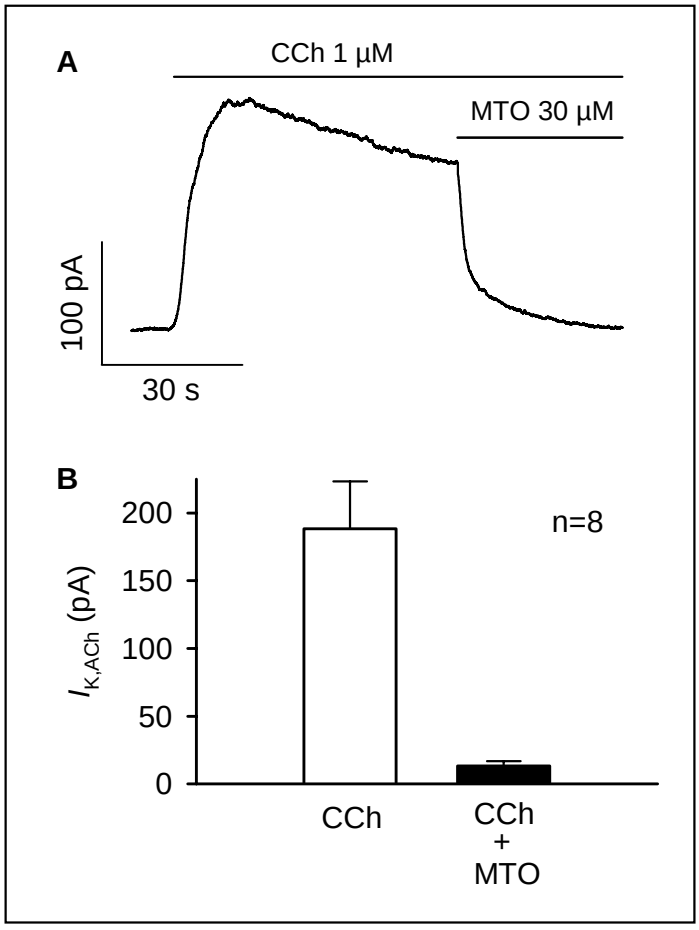

Figure 20. Inhibiton of $I_{K,ACh}$ by MTO in guinea-pig atrial myocytes. The membrane potential of the cells were continuously clamped at -50 mV, and $I_{K,ACh}$ was induced by 1 µM carbamylcholine (CCh). A, a typical original current recording showing the inhibitory effect of 30 µM MTO on $I_{K,ACh}$. B, summary of the inhibitory effect of 30 µM MTO on $I_{K,ACh}$. Data from the same cell group are compared.

Muscarinic receptors couple with K_{ACh} channels through a pertussis toxin-sensitive class of GTP-binding proteins in atrial cells (Pfaffinger *et al*., 1985). When a nonhydrolysable GTP analogue such as guanosine-5'-*O*-(3-thiotriphosphate), GTPγS, is applied intracellularly,

activation of GTP-binding proteins occurs and induces a persistent activation of K_{ACh} channels which is resistant to inhibition by muscarinic receptor antagonists (Breitwieser and Szabo, 1985). With 100 µM GTPγS in the recording pipette, there was a continuous rise of a K^+ outward current in guinea-pig atrial cells clamped at -50 mV (Figure 21A). This current reached its maximum in 10 min and remained stable thereafter. Contrary to CCh, MTO induced only a very weak (9%) but reversible inhibition of the current evoked by GTPγS. In five cells loaded with GTPγS, the K^+ current increased to 361.4 ± 29.3 pA and MTO reversed this current to 314.4 ± 47.5 pA, i.e. by 12.6% (Figure 21B). Although the experiment clearly shows that the predominant action of MTO on $I_{K,ACh}$ is via muscarinic receptors, a small direct inhibitory effect on K_{ACh} channels seems to contribute.

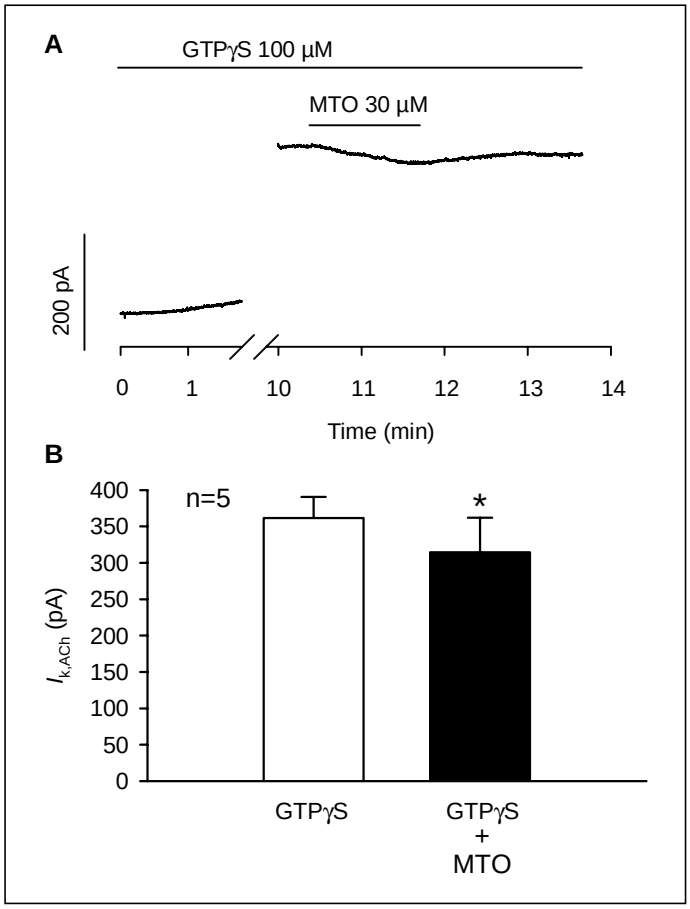

Figure 21. Effect of MTO on $I_{K,ACh}$ elicited by GTPγS in guinea-pig atrial myocytes. GTPγS was loaded into the cells through a patch pipette for 10 min. A, original recording showing slight inhibition of $I_{K,ACh}$ by 30 µM MTO in a typical cell dialyzed with 100 µM GTPγS. B, summary of the effect of 30 µM MTO on $I_{K,ACh}$ induce by 100 µM GTPγS. *, $p<0.05$ versus GTPγS alone.

4.6 [^{3}H]-QNB binding study

Binding of [^{3}H]-QNB to a preparation of human atrial membranes is shown in Figure 22A. The binding was saturable between 500 and 1000 pM. Scatchard analysis (Figure 22B) indicated a homogenous population of binding sites, a B_{max} of 434 fmol/mg protein and a K_D of 234 pM. In the presence of 30 µM MTO, binding of [^{3}H]-QNB was almost completely abolished (Figure 23A). MTO concentration-dependently displaced [^{3}H]-QNB from its binding sites with calculated equilibrium dissociation constants (K_i) of 1.29, 1.10 and 1.02 µM at 0.70, 1.48 and 2.91 nM [^{3}H]-QNB, respectively (Figure 23B).

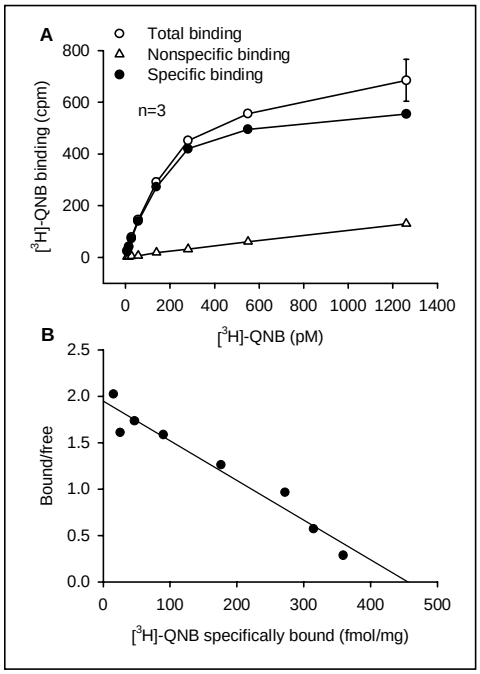

Figure 22. [^{3}H]QNB binding to washed membranes from human atrial tissues. A, saturation isotherm of [^{3}H]QNB binding. The nonspecific binding was measured in the presence of 1 µM atropine, whereas the specific binding was calculated by subtracting the nonspecific binding from the total binding. B, scatchard plot of the specific [^{3}H]QNB binding data depicted in A. Data are mean values taken from a representative experiment carried out in triplicate.

Figure 23. Antagonistic effect of MTO on [^{3}H]-QNB binding to washed membranes from human atrial tissues. A, block of the total [^{3}H]-QNB binding by 30 µM MTO. Data are mean values taken from a representative experiment carried out in triplicate. B, displacement of specific [^{3}H]-QNB binding by MTO. MTO was added at concentrations ranging from 0.1 to 1000 µM in the presence of three different [^{3}H]-QNB concentrations. Fitted curves are representative of two independent experiments carried out in triplicate. Correlation coefficients of the fits are 0.99, 0.96 and 0.97 in the presence of 0.7, 1.48 and 2.91 nM [^{3}H]-QNB, respectively.

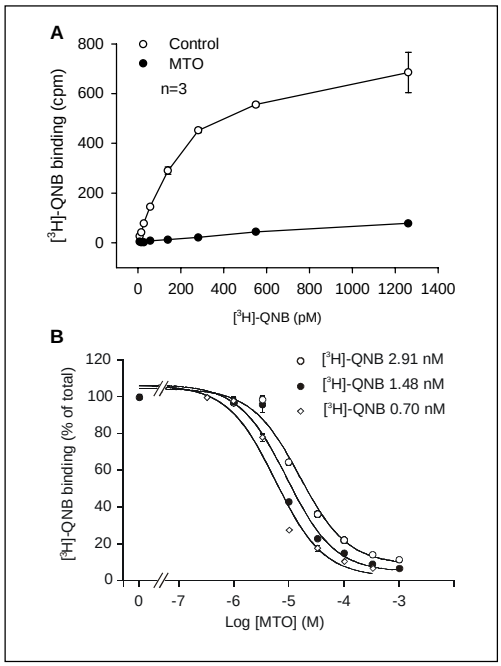

4.7 Force of contraction in guinea-pig papillary muscles

In isometrically contracting guinea-pig papillary muscles mitoxantrone (MTO) produced a concentration- and time-dependent positive inotropic effect (Figure 24). The positive inotropic effect developed slowly over several hours (Figure 24A). With 30 µM MTO, the increase in force of contraction became visible after a latency of 30 min and was significant compared with the pre-drug control value after 1 h ($p < 0.05$). After 4 h, force had increased about 3-fold from 1.4 ± 0.2 (control) to 4.1 ± 0.5 mN (n = 8; Figure 24B). When 10 µM MTO was applied to the bath solution, the positive inotropic effect became significant only after 3 h, and after 4 h force of contraction had increased by 58% from 1.2 ± 0.1 (control) to 1.9 ± 0.3 mN (n = 5; Figure 24B). Similar positive inotropic effects of MTO were observed when the muscles had been pretreated for 30 min with 10 µM TTX (not shown). 30 µM MTO increased the force of contraction by 1.6-fold within 4 h (from 0.9 ± 0.1 to 2.4 ± 0.3 mN, n=3, $p<0.05$). Experiments carried out in the absence of MTO showed a continuous decline in the force of contraction over time. After 4 h, force had decreased to 81.2 ± 5.5 % of the control level (n = 6).

The MTO-induced increase in force of contraction was accompanied by a marked prolongation of contraction duration. As shown in Figure 24A and 24C, this effect was due to

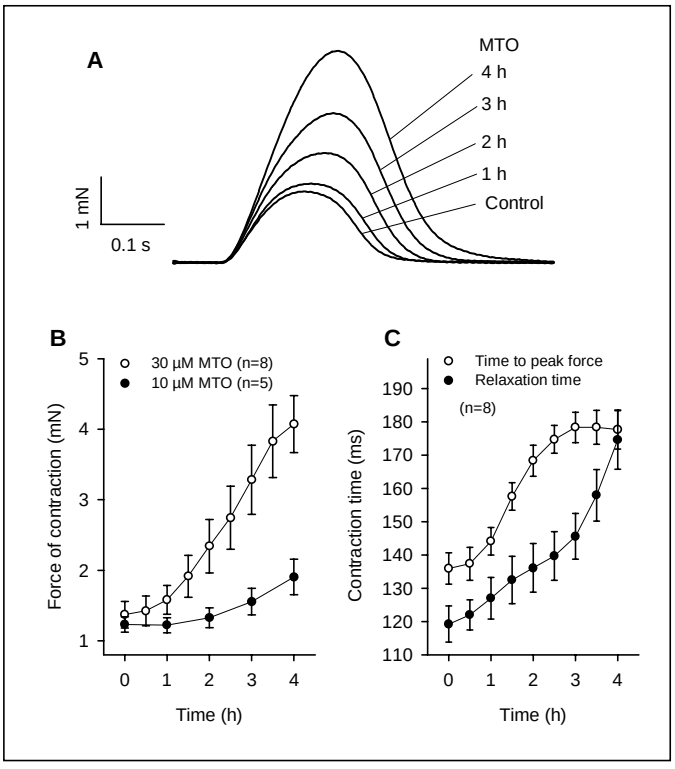

Figure 24. Time-dependent positive inotropic effect induced by MTO in guinea-pig papillary muscle. Muscles were electrically stimulated at 0.5 Hz with the resting tension kept constant at 4 mN. A, superimposed original recordings showing the effects of 30 µM MTO on isometric force of contraction in a typical muscle. B, summary of the time course of the positive inotropic effect of 10 and 30 µM MTO. C, time-dependent increase of time to peak force and of relaxation time in the presence of 30 µM MTO.

a prolongation of time to peak force and of relaxation time. Both time parameters were significantly prolonged after 1 h of incubation with 30 µM MTO ($p<0.05$). In eight papillary muscles, time to peak force and relaxation time increased within 4 h from 136 ± 5 and 119 ± 6 ms (control values) to 178 ± 5 (by 31%) and 175 ± 9 ms (by 47%), respectively. When papillary muscles were exposed to 30 µM MTO for more than 4 h, some preparations developed slowly rising contractures which usually terminated the positive inotropic effect. The contracture developed much faster when higher concentrations of MTO (>30 µM) were used. In Figure 25, the effect of 60 µM MTO on resting tension of the papillary muscles was demonstrated. Figure 25A shows superimposed original contraction recordings from a representative muscle. The resting tension of this muscle increased after 3 h of incubation in 60 µM MTO from a control value of 4.0 mN to 5.0 mN. After 4 h, resting tension further increased to 6.1 mN, whereas peak force of contraction declined. In Figure 25B, the time-dependent changes in force of contraction and resting tension induced by 60 µM MTO in seven muscles are summarized. During the first 2.5 h of incubation, MTO caused a time-dependent positive inotropic effect without significantly changing the resting tension. The force of contraction increased to 189.7 ± 12.9% of the control within 2.5 h. Then, the resting tension started to increase which gradually diminished the positive inotropic effect. After 5 h of incubation, the resting tension amounted to 142.1 ± 8.2% of the control value. At the same time, the force of contraction was only 109.7 ± 9.6% that of the control level.

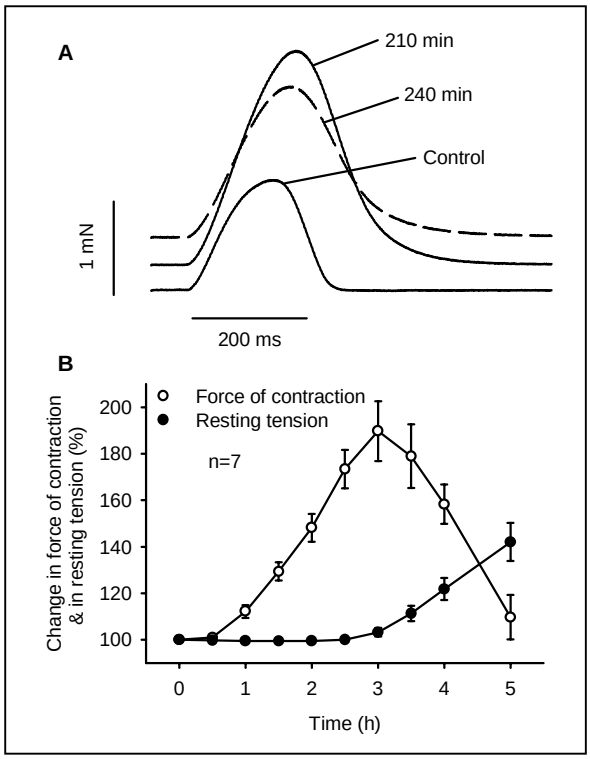

Figure 25. Effect of 60 µM MTO on resting tension in guinea-pig papillary muscles. Muscles were electrically stimulated at 0.5 Hz. A, superimposed original contraction traces recorded from a typical muscle showing increase in resting tension caused by MTO. B, summary of the time-dependent changes of the contraction force and resting tension in the presence of MTO.

4.8 Cell shortening and action potential duration

When the effects of MTO on cell shortening was investigated in isolated ventricular myocytes that had been current-clamped at 0.5 Hz, similar results as those obtained in papillary muscles were observed. Figure 26A shows superimposed original recordings from a typical experiment, superfusion of a cell with 30 µM MTO produced a time-dependent prolongation of APD accompanied by an enhancement and prolongation of cell shortening. APD_{90} increased from 221 ms (control) to 260 and to 391 ms, whereas cell shortening rose from 9.2 µm (control) to 15.8 and 20.5 µm after 30 and 50 min, respectively. Simultaneously, time to peak shortening and relaxation time were prolonged from 128 and 124 ms (control) to 135 and 151 ms at 30 min and to 140 and 170 ms after 50 min. In nine cells, in which the shortening could be followed continuously over 30 min, MTO induced a 77% increase of cell shortening from 6.0 ± 0.6 (control) to 10.6 ± 1.1 µm (Figure 26B). Shortening duration was prolonged by 24% from 263 ± 25 to 325 ± 29 ms (Figure 26C). APD_{90} of these cells was prolonged by 19% from 254 ± 16 to 301 ± 19 ms. Shortening of control cells which were not exposed to MTO decreased slightly (by 9.5%) but significantly within 30 min from 7.2 ± 1.0 to 6.8 ± 0.9 µm (n=7; Figure 26B), whereas shortening duration was not affected (Figure 26C).

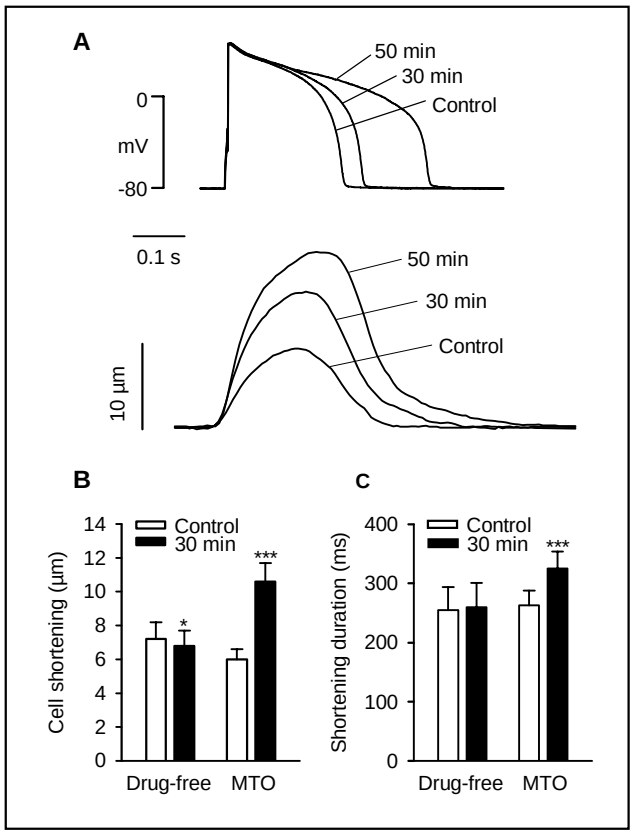

Figure 26. Effects of MTO on cell shortening and APD in current-clamped guinea-pig ventricular myocytes. Stimulation frequency 0.5 Hz. A, superimposed original recordings showing the time-dependent increase of APD (upper traces) and cell shortening (lower traces) in the presence of 30 µM MTO. Amphotericin B (300 µg/ml) was included in the electrode solution to permeabilize the membrane patch. The action potential and cell shortening were measured simultaneously in the same cell. B and C, summary of the changes in peak amplitude of cell shortening (B) and shortening duration (C) within 30 min either in the absence (drug-free, n=7) or in the presence of 30 µM MTO (n=9). *, $p<0.05$; ***, $p<0.001$ versus the respective control.

In order to investigate the influence of APD on cell shortening, myocytes were AP-clamped at various APDs. Figure 27A (upper traces) shows two superimposed action potentials which were obtained from a cell before (a) and 1 h after superfusion with 30 µM MTO (b). Recorded action potentials served then as voltage-commands to clamp another cell in order to elicit corresponding contractions (lower traces in Figure 27A). It can be seen that a prolongation of APD_{90} from 258 (a) to 433 ms (b) was accompanied by an enhancement of cell shorting from 3.9 (a) to 6.1 µm (b). Shortening of the first contraction after APD prolongation was not changed but increased during the following contractions. Time to peak shortening was slightly decreased from 164 to 159 ms by APD prolongation while relaxation followed a more complex time course. Relaxation developed an inflection, so that a rapid relaxation phase which dominated about 75% of total cell shortening was followed by a tail which was markedly slowed by the prolonged APD. Figure 27B shows the relation between the percent increase of APD_{90} and the respective change of cell shortening obtained from eight cells. Prolonging APD_{90} by 24, 48 and 68 % from a control value of 258 ms resulted in an increase of cell shortening by 12.8 ± 2.1, 27.6 ± 4.0 and 35.0 ± 6.6 %, respectively. In these cells, the time to peak shortening was significantly decreased from a control value of 138 ± 8 to 135 ± 8 (by 2.2%, $p<0.05$), 130 ± 8 (by 5.8%, $p<0.001$) and 128 ± 8 ms (by 7.2%, $p<0.001$) when APD_{90} was prolonged by 24, 48 and 68%, respectively.

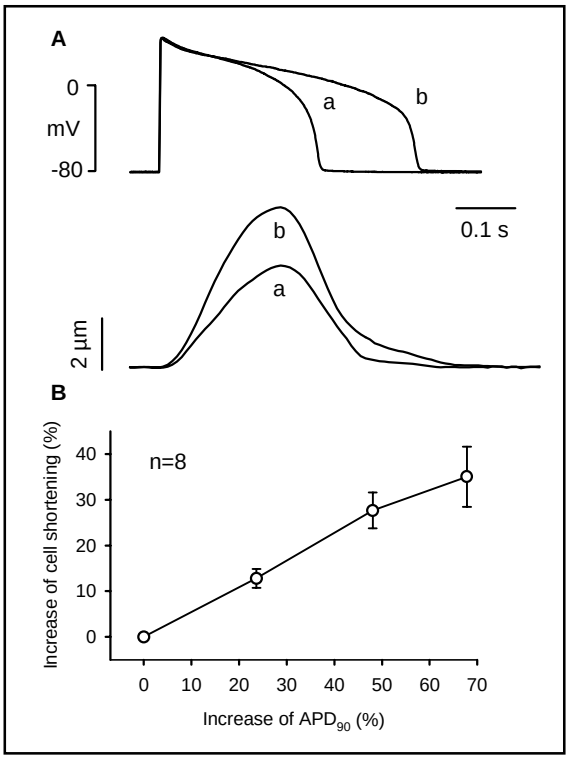

Figure 27. Increase of cell shortening induced by prolongation of APD in guinea-pig ventricular myocytes clamped with action potentials of various duration. The action potentials had been recorded before from a myocyte at different times during its exposure to 30 µM MTO. These action potentials served then as voltage-commands for other cells to trigger contraction at 0.5 Hz.

To investigate whether MTO enhanced cell shortening independent of APD prolongation, ventricular myocytes were AP-clamped with an action potential of constant duration. In the experiment shown in Figure 28A, a cell was AP-clamped at 0.5 Hz with an APD_{90} of 258 ms. Application of 30 µM MTO to the superfusing solution resulted in an increase in cell shortening from 6.4 (control) to 7.8 and 9.6 µm after 20 and 30 min, respectively. This increase was accompanied by a prolongation of time to peak shortening and of relaxation time from 158 and 108 ms (control) to 162 and 132 ms after 20 min and to 184 and 156 ms after 30 min, respectively. A summary of the results is shown in Figure 28B and 28C. 30 µM MTO enhanced the shortening of six cells by 59% from 7.1 ± 1.2 to 11.3 ± 1.2 µm and prolonged shortening duration by 22% from 252 ± 6 to 307 ± 12 ms after 30 min. In five control cells which were not exposed to MTO, cell shortening decreased significantly within 30 min by 10% from 7.2 ± 0.5 to 6.5 ± 0.3 µm (Figure 28B), whereas shortening duration did not change (Figure 28C).

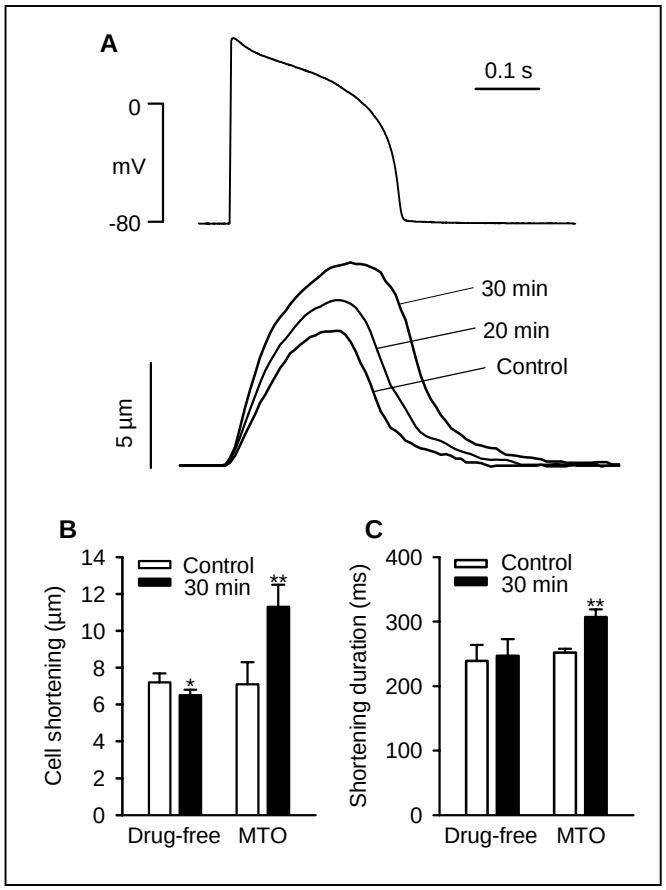

Figure 28. Time-dependent increase of cell shortening induced by MTO in guinea-pig ventricular myocytes clamped with a constant action potential. The action potential (APD_{90} = 258 ms) had been recorded before from a myocyte in the absence of MTO, and was then used as a voltage-command for other cells to trigger contraction at 0.5 Hz. A, superimposed original recordings showing the time-dependent increase of cell shortening induced by 30 µM MTO (lower traces) in a myocyte clamped at a constant APD (upper trace). B and C, summary of the changes in the peak amplitude of cell shortening (B) and shortening duration (C) after 30 min either in the absence (drug-free, n=5) or in the presence of 30 µM MTO (n=6). *, $p<0.05$; **, $p<0.01$ versus the respective control.

4.9 Action potential duration and Ca^{2+} transients

In order to determine the influence of APD and of MTO on intracellular Ca^{2+} transients, myocytes were AP-clamped with action potentials of various duration. The original recordings of Figure 29A show action potentials (upper traces) which had been recorded before at different times from a myocyte exposed to 30 µM MTO. The recorded action potentials served then as voltage-commands for another cell to elicit the Ca^{2+} transients (lower traces). It can be seen that the stepwise prolongation of APD is accompanied by an increase of the peak of the respective Ca^{2+} transient. As in the contraction experiments, 3 to 4 action

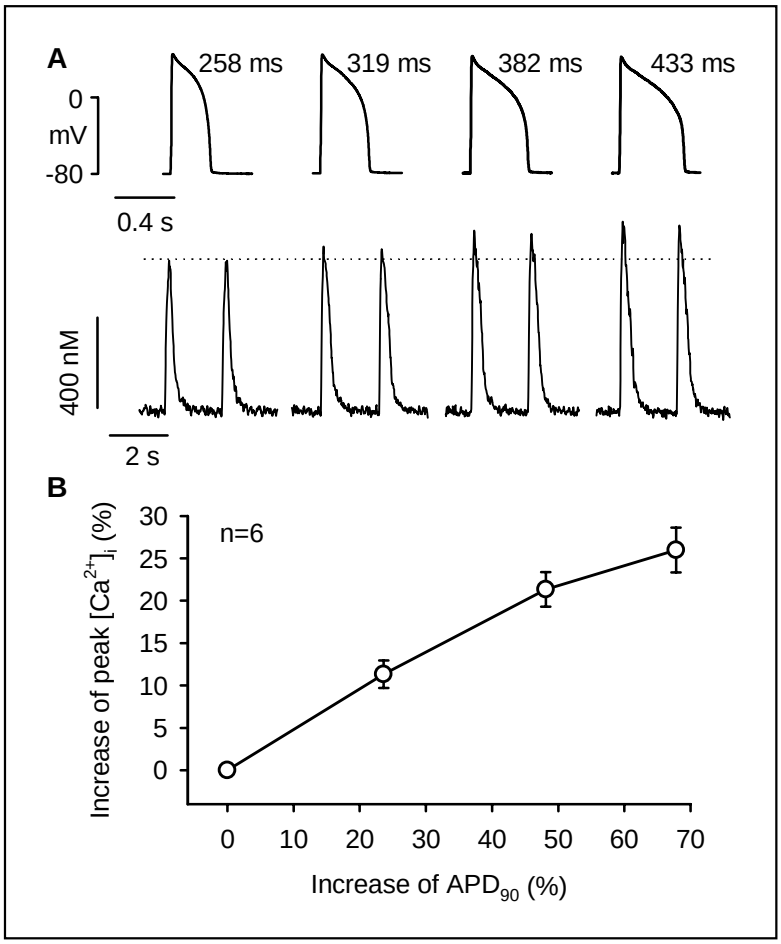

Figure 29. Increase of intracellular Ca^{2+} transients induced by prolongation of APD in guinea-pig ventricular myocytes clamped with action potentials of various duration. The action potentials had been recorded before from a myocyte at different times during its exposure to 30 µM MTO. These action potentials were then used as voltage-commands for other cells to elicit Ca^{2+} transients at 0.5 Hz. The Ca^{2+} transients were measured by loading the cells with 30 µM fura-2 pentasodium salt through the patch pipette. A, original traces showing the commanding action potentials (upper panel) and the corresponding Ca^{2+} transients (lower panel). The values of APD_{90} are indicated in ms. B, relation between percent increase of APD_{90} and the respective change of the peak Ca^{2+} transients. The control values for APD_{90} and peak amplitude of Ca^{2+} transients were 258 ms and 607 ± 52 nM, respectively.

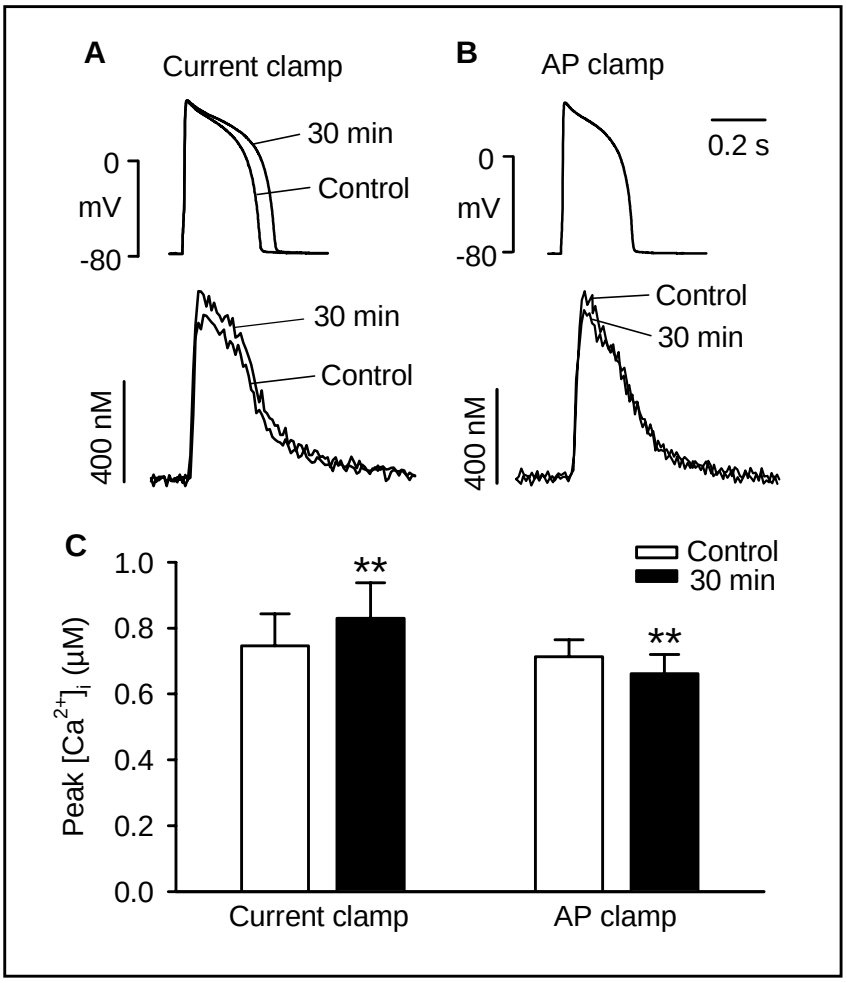

Figure 30. Effects of MTO on intracellular Ca^{2+} transients in guinea-pig ventricular myocytes under current clamp or AP clamp. The Ca^{2+} transients were measured by loading the cells with 30 µM fura-2 pentasodium salt through the patch pipette. A, superimposed original recordings showing simultaneous increase of APD (upper traces) and Ca^{2+} transients (lower traces) 30 min after superfusing a current-clamped myocyte with 30 µM MTO. The stimulation frequency was 0.5 Hz. B, original recordings showing the effect of 30 µM MTO (30 min) on Ca^{2+} transients (lower traces) in a cell clamped with a constant APD (upper trace) at 0.5 Hz. The commanding action potential (APD_{90} = 258 ms) had been recorded before from a different myocyte. C, summary of the effects of 30 µM MTO (30 min) on peak Ca^{2+} transients under either current clamp (n=6) or constant AP-clamp (n=5). ** $p<0.01$ versus the respective control.

potentials were necessary to obtain a steady-state increase in the amplitude of the Ca^{2+} transient. Figure 29B summarizes the results obtained in six cells, prolongation of APD_{90} by 24, 48 and 68% increased the peak of the Ca^{2+} transient by 11.3 ± 1.6, 21.3 ± 2.0 and 26.0 ± 2.6%, respectively. When a myocyte was current-clamped at 0.5 Hz and superfused with 30µM MTO for 30 min, APD_{90} increased by 26% from 274 to 345 ms and the simultaneously

evoked Ca^{2+} transient rose by 13% from 656 to 741 nM (Figure 30A). The summary of the results from six cells demonstrates a significant increase in peak $[Ca^{2+}]_i$ by 10% from 746 ± 97 to 822 ± 104 nM (Figure 30C, left panel). In contrast, when a myocyte was AP-clamped with constant APD (APD_{90} = 258 ms), 30 µM MTO produced within 30 min a small decline of peak $[Ca^{2+}]_i$ from 788 to 734 nM (Figure 30B). The combined data obtained from five cells showed a significant decrease in Ca^{2+} transients by 7.2% from 713 ± 52 to 662 ± 58 nM (Figure 30C, right panel). In control cells which were not treated with MTO, peak Ca^{2+} transients decreased slightly within 30 min from 701 ± 67 to 657 ± 69 nM (by 6.3%, n=5, $p<0.05$) under current clamp condition and from 669 ± 93 to 631 ± 89 nM (by 5.7%, n=4, $p<0.05$) under AP clamp condition.

5. Discussion

The present study describes the acute effects of the anticancer drug mitoxantrone (MTO) on the contractility, membrane electrical properties and the muscarinic receptor of isolated cardiac preparations. The most prominent effects of MTO include: (1) time-dependent prolongation of action potential duration (APD); (2) blockade of muscarinic receptors; (3) a time- and concentration-dependent positive inotropic effect with attenuation of muscle relaxation.

5.1 Mechanisms of prolongation of action potential duration by mitoxantrone

In principle, both an increase in depolarizing inward currents during the plateau phase of action potential and a decrease in hyperpolarizing outward currents can cause prolongation of APD. In guinea-pig ventricular myocytes, the main inward currents which determine APD are the L-type Ca^{2+} current ($I_{Ca(L)}$) and the non-inactivating Na^+ window current. The major outward currents involved in the regulation of APD include the delayed rectifier K^+ current (I_K) and the inward rectifier K^+ current (I_{K1}). In other species, such as human or rat ventricles, the transient outward current (I_{to}) also plays an important role in the repolarization process.

5.1.1 Role of Na^+ and Ca^{2+} inward currents

In order to find out whether a window current flowing through Na^+ channels was influenced by MTO, tetrodotoxin (TTX) was used in the present experiments. TTX is a highly selective Na^+ channel blocker (Narahashi 1974). At a concentration of 10 µM, TTX has been shown to effectively antagonize the APD-prolonging effect of several Na^+ channel activators in guinea-pig ventricular muscle (Honerjäger 1982). If APD prolongation induced by MTO would have been due to an activation of Na^+ channels, this effect would have been inhibited in the presence of 10 µM TTX. The finding that the APD-prolonging effect of MTO still persisted in cells pre-treated with TTX argue against an involvement of the Na^+ window current in the MTO-induced APD prolongation.

The possibility that the MTO-induced APD prolongation might have arisen from an enhancement of $I_{Ca(L)}$ was tested by direct measurement of this type of current with the whole-cell voltage-clamp technique. The results showed that neither the peak amplitude nor the inactivation kinetics of $I_{Ca(L)}$ were affected by MTO. Thus, $I_{Ca(L)}$ does not seem to play any significant role in the APD-prolonging effect of MTO.

5.1.2 Role of delayed rectifier K^+ current

Delayed rectifier K^+ channels play a key role in regulating cardiac APD. In guinea-pig ventricular myocytes, I_K is composed of two components, a rapidly activating, inward rectifying component, I_{Kr}, and a slowly activating component, I_{Ks} (Sanguinetti and Jurkiewicz, 1990a). At normal heart rates, both components of I_K seem to contribute to repolarization of the cardiac action potential (Sanguinetti and Jurkiewicz, 1990a; Heath and Terrar, 1996). I_{Ks} has been shown to be more dominant than I_{Kr} during the plateau phase of action potential, whereas I_{Kr} is more important than I_{Ks} during phase 3 of the action potential (Sanguinetti and Jurkiewicz, 1990a; Zeng *et al*., 1995). Although I_{Kr} is the target of most clinically used class III antiarrhythmic drugs (Sanguinetti and Jurkiewicz, 1990a; Katritsis and Camm, 1993), selective blockers of the I_{Ks} channel complex have been developed recently and their APD prolonging effect has been clearly demonstrated (Busch *et al*., 1996; Salata *et al*., 1996, Schreieck *et al*., 1997).

Although the two components of I_K were not separately measured in most of our experiments, some of the findings are compatible with the view that MTO preferentially blocked I_{Kr}. Because I_{Kr}, by fast inactivation of channels from open state (Shibasaki, 1987; Spector *et al*, 1996; Yang *et al*., 1997), exhibits inward rectification at positive potentials (0 to +40 mV), a specific I_{Kr} blocker should have no effect on time-dependent outward currents elicited at voltages above + 40 mV when I_{Kr} is almost completely inactivated (Sanguinetti and Jurkiewicz, 1990a). This is exactly what was found with MTO, the time-dependent outward current measured at the end of 1s pulses was only suppressed at voltages during which I_{Kr} was measurably activated (see Figure 10).

Analysis of activation of I_K is difficult because of additional currents which may be simultaneously activated by depolarizing pulses. Upon repolarization from activating voltage steps, an outward tail current is observed which is thought to represent the slow deactivation of I_K and serves as a more reliable index of the I_K current (Heath and Terrar, 1996). With repolarizing steps, inactivated channels conducting I_{Kr} rapidly enter the open state, from which channels close slowly, thereby also contributing to the peak and the decay of I_K tail currents elicited upon repolarization from very positive potentials (Shibasaki, 1987). Because I_{Ks} slowly activates with depolarization over a time course of many seconds, its contribution to I_K tail current increases over time and should therefore render peak I_K tail current more resistant to blockers of I_{Kr} at longer pulse durations. MTO suppressed I_K tail currents at all voltages (-30 to +70 mV) and, consistent with I_{Kr} block, suppression decreased at voltages

above +20 mV and this decrease was more pronounced with long (1s) as compared with short pulses (250 ms).

Although the above results strongly suggested that MTO preferentially inhibited I_{Kr} , direct proof for this inhibition came from experiments carried out in nominally Ca^{2+}-free bath solution. It has been demonstrated that under this condition, I_{Kr} could be separated from I_{Ks} because the activating potentials of both currents were shifted in opposite direction (Sanguinetti and Jurkiewicz, 1990b; Jurkiewicz and Sanguinetti, 1993). When I_{Kr} was elicited by a 500-ms depolarizing pulse to -10 mV from a holding potential of -40 mV, MTO significantly inhibited both the steady-state- and the tail current.

Specific blockers of I_{Kr} such as d-sotalol or dofetilide have been reported to display reverse rate-dependent effects, i.e., they prolong APD more at long than at short cycle lengths (Tande *et al*., 1990; Gwilt *et al*., 1991; Jurkiewicz and Sanguinetti, 1993; Gjini *et al*., 1996). In the present study we found that MTO also displayed reverse rate-dependence, its APD prolonging action in guinea-pig papillary muscle was almost completely abolished by increasing the stimulation frequency to 4 Hz. In this context, it is interesting to note that specific inhibitors of I_{Ks} such as chromanol 298B and blockers of both I_{Kr} and I_{Ks} such as ambasilide or amiodarone produced frequency-independent effects on APD (Bosch *et al*., 1997; Salata *et al*., 1996; Schreieck *et al*., 1997), indicating that reverse rate-dependence of APD prolongation is a characteristic feature of pure I_{Kr} blocking drugs. There are several explanations for reverse rate-dependence such as accumulation of I_{Ks} at high frequencies when cycle length becomes shorter than I_{Ks} deactivation time (Sanguinetti and Jurkiewicz, 1990a; Jurkiewicz and Sanguinetti, 1993), $[Ca^{2+}]_i$-dependent increase in I_{Ks} at high stimulation rates (Hiraoka *et al*., 1995) and a decreased sensitivity of I_{Kr} at high $[K^+]_o$, due to accumulation of K^+ close to the outer cell membrane during rapid stimulation (Attwell *et al*., 1981; Yang and Roden, 1996). It should be noted, however, that none of these mechanisms has been firmly established as the cause of reverse rate-dependence of APD by I_{Kr} blockers.

A striking property of I_{Kr} is its unusual sensitivity to changes in $[K^+]_o$ (Yang and Roden, 1996; Yang *et al*., 1997). Thus I_{Kr} plays a major role causing shortening of APD when $[K^+]_o$ is elevated or, conversely, prolongation of APD when $[K^+]_o$ is reduced. Accumulation of $[K^+]_o$ in extracellular clefts of contracting guinea-pig papillary muscles may therefore be responsible for the smaller effect of MTO on APD in multicellular preparations as compared with single cells (see Figures 5 and 7). APD prolongation by block of I_{Kr} is an important factor in arrhythmogenesis (for review, see Sanguinetti and Salata, 1996). Although early afterdepolarizations by MTO were only observed in single cardiomyocytes, I_{Kr} block may

also cause undesirable proarrhythmic effects in multicellular heart preparations, especially when $[K^+]_o$ is low.

5.1.3 Role of inward rectifier K^+ current

The observation that MTO did not alter resting membrane potential does not by itself exclude an inhibitory effect on I_{K1} because only a fraction of the normal I_{K1} is required to maintain the membrane potential near E_K during diastole. Indeed, current-voltage relations disclosed a significant reduction by MTO of the outward current hump observed at potentials between -70 and -30 mV. This effect was probably due to inhibition of I_{K1} because this current is primarily activated over this voltage range in guinea-pig ventricular myocytes (Backx and Marban, 1993), and MTO had no influence on the residual background currents when I_{K1} was blocked by 1 mM $BaCl_2$. During the plateau of the cardiac action potential, channels conducting I_{K1} allow either no or very little current to pass. However, when the cell repolarizes and especially during the final repolarization, I_{K1} becomes important and is responsible for the regenerative increase in repolarization rate (Shimoni *et al*., 1992; Zeng *et al*., 1995). Whether blockade of I_{K1} induces action potential prolongation is an unsettled issue, because "pure" I_{K1} blockers such as the benzopyran compounds RP 58866 and its active enantiomer terikalant, turned out to be also potent blockers of I_{Kr} (Jurkiewicz *et al*., 1996).

Interestingly, in the rat cardiomyocyte where rapid repolarization of action potential is due to activation of the transient outward current, I_{to}, (Josephson *et al*., 1984; Dukes and Morad, 1991) MTO had no influence on APD as long as this outward current was dominant. During late repolarization, however, when I_{K1} becomes activated, MTO markedly delayed final repolarization which eventually resulted in early afterdepolarizations. To what extent inhibition of I_{K1} by MTO contributes to APD prolongation in guinea-pig myocytes is presently not known.

5.2 Antimuscarinic effects of mitoxantrone

Normally the heart is under the steady control of the sympathetic and parasympathetic autonomic nervous system. The parasympathetic transmitter acetylcholine antagonizes the effects of catecholamines on force of contraction, heart rate and AV-conduction. One important mechanism by which catecholamines and acetylcholine exert their antagonistic effects is by modulating $I_{Ca(L)}$. Although MTO had no direct effect on $I_{Ca(L)}$, it influenced the current indirectly by reversing the inhibitory action of carbamylcholine on isoproterenol-stimulated $I_{Ca(L)}$. This effect could have been due to inhibition of muscarinic receptors or to a

mechanism downstream to receptor activation. The A_1-adenosine receptor agonist R-PIA utilizes the same pertussis toxin-sensitive intracellular signal transduction pathway as carbamylcholine to inhibit the catecholamine-enhanced $I_{Ca(L)}$ (for review see Belardinelli et al., 1989). Since MTO did not affect $I_{Ca(L)}$ in the presence of R-PIA plus isoproterenol, inhibition of muscarinic receptors was very likely the mechanism of MTO's indirect effect on $I_{Ca(L)}$.

In atrial cells as well as in sinoatrial- and atrioventricular node, activation of K_{ACh} channels by an increased vagal tone plays an important role in slowing sinus rate, prolonging A-V conduction and shortening atrial refractoriness. K_{ACh} channels are linked to muscarinic or adenosine receptors through pertussis-toxin sensitive GTP-binding proteins (Pfaffinger *et al*., 1985) and it has been shown that GTPγS, a nonhydrolysable GTP analogue, can activate GTP-binding proteins irreversibly, resulting in persistent activation of K_{ACh} channels (Kurachi *et al*., 1986). MTO (30 µM) decreased the carbamylcholine-activated $I_{K,ACh}$ in control cells by more than 90% but reversed the $I_{K,ACh}$ activated by GTPγS by only 12%. This finding suggests that MTO may act primarily through its blocking action on muscarinic receptors and only to a small extent by blocking the K_{ACh} channel itself and/or by interfering with the regulatory functions of GTP-binding proteins coupled to the channel.

The blocking effect of MTO on cardiac muscarinic receptors was further confirmed by radioligand binding experiments which showed that MTO displaced [^{3}H]-QNB binding concentration-dependently (1 to 1000 µM). The slightly different K_i values obtained at various [^{3}H]-QNB concentrations indicate that this antagonistic effect was not strictly competitive.

The heart rate is predominantly under the parasympathetic control. Thus administration of MTO which blocks the muscarinic receptors of the parasympathetic transmitter acetylcholine, can be expected to raise the heart rate in vivo. On the one hand, this effect should alleviate APD prolongation of ventricular myocytes due to reverse rate-dependence. On the other hand, inhibition of the muscarinic receptors by MTO may facilitate afterdepolarizations due to the dominance of sympathetic activity.

5.3 Mechanisms of the positive inotropic effect of mitoxantrone

5.3.1 Role of action potential duration

The positive inotropic effect of MTO was accompanied by a progressive prolongation of APD implying that both effects could be related to each other. It should be noted that blockers of I_{Kr} such as sotalol, dofetilide and E-4031 have also been shown to produce positive

inotropic effects presumably as a result of the prolonged action potential (Tande et al., 1990; Wettwer et al., 1991).

It is well known that an increase in APD particularly at the plateau level is associated with an increase in contraction force (Morad and Trautwein, 1968; Terrar and White, 1989). The increased inotropic response to action potential prolongation may be the result of a reduction in the driving force for Ca^{2+} extrusion via the Na^{+}-Ca^{2+} exchange and/or due to a prolonged Ca^{2+} influx via noninactivated Ca^{2+} channels. Because both these mechanisms are voltage-dependent, prolongation of APD will increase the Ca^{2+} content of the SR and thus the size of the contraction.

When action potentials recorded in the presence of MTO served as voltage-commands for MTO-naive cells, prolonged APDs resulted in an increase in cell shortening and in a small decrease of the time to peak shortening. Both effects developed over several beats, indicating that with each depolarization more Ca^{2+} is available for uptake into the SR and for subsequent release. Initiation of relaxation was barely affected by APD, relaxation proceeded with high speed to about 25% of the peak amplitude but became then progressively slower until final repolarization of the action potential terminated the residual shortening. A similar biphasic decrease of cell contraction and of intracellular Ca^{2+} transients during long lasting depolarizing steps has been described in cardiac myocytes of several species (Bridge et al., 1988; Bers and Bridge, 1989; Bers et al., 1990). It was proposed that the voltage-independent relaxation is probably due to rapid Ca^{2+} sequestration by the SR which increases with the cytosolic Ca^{2+}concentration, whereas the voltage-dependent relaxation reflects the ceasing of the Ca^{2+} influx and the enhancement of Ca^{2+} extrusion via Na^{+}-Ca^{2+} exchange.

5.3.2 Role of other intracellular Ca^{2+} regulating systems

In comparison with control cells which were clamped with action potentials of various duration (Figure 27), myocytes exposed to MTO responded with a stronger shortening at a comparable APD, accompanied by a prolongation of time to peak shortening and of relaxation time (Figure 28). Evidence that MTO produced a positive inotropic effect which was in part independent of APD prolongation evolved from the finding that MTO enhanced the shortening of myocytes which were AP-clamped with a constant APD. In these cells a significant prolongation of contraction duration was also observed.

Mechanisms by which MTO could have increased force of contraction beyond the level of APD prolongation are an enhancement of the transmembrane Ca^{2+} current via voltage-gated L-type Ca^{2+} channels either by cyclic AMP accumulation or by direct modulation of channel

gating and elevation of intracellular Na^+ activity either by inhibiting Na^+-K^+ pump or by increasing transmembrane Na^+ influx (Varro and Papp, 1995). Drugs which increase intracellular cyclic AMP levels, such as ß-adrenoceptor agonists or inhibitors of phosphodiesterase, enhance Ca^{2+} influx via L-type Ca^{2+} channels and stimulate the activity of the SR Ca^{2+} pump which becomes functionally effective as a shortening of relaxation time (Raffaeli et al., 1989; Brixius et al., 1997). The finding that MTO prolonged relaxation time and had no influence on L-type Ca^{2+} current excludes cyclic AMP-dependent pathways and a direct channel modulation. In addition, the positive inotropic effect of cardioactive steroids which is due to inhibition of Na^+-K^+ pump is not accompanied by a prolongation of contraction (Reiter, 1972). Prolongation of relaxation time accompanies the positive inotropic effect of many drugs and toxins which increase transmembrane Na^+ influx (Honerjäger, 1982; Buggisch et al., 1985). In contrast to the Na^+ channel modulators, inotropic effects as well as APD prolongation of MTO were not influenced by the Na^+ channel blocker TTX.

Recently, the anthracycline derivative doxorubicin, another highly effective antineoplastic agent, was demonstrated to produce a slowly developing positive inotropic effect in guinea-pig papillary muscles (Wang and Korth, 1995). MTO and doxorubicin are both anthraquinone-based compounds and there are similarities between both compounds such as positive inotropic effect and APD prolongation but also striking differences in their cardiac actions. Despite its strong positive inotropic effect, doxorubicin markedly reduced contraction velocity and prolonged the time to peak force. This effect resembles the action of ryanodine in cardiac cells (Lewartowski et al., 1990) and is due to an increase of the open probability of Ca^{2+} release channels in the SR (Nagasaki and Fleischer, 1989; Holmberg and Williams, 1990; Wang and Korth, 1995). Reports on the action of MTO on SR Ca^{2+} channels are conflicting (Abramson et al., 1988; Holmberg and Williams, 1990; Kim et al., 1994), but the present experiments do not support a doxorubicin or ryanodine-like action of MTO on SR function. The possibility, however, that the moderate prolongation of time to peak shortening is the manifestation of a weak effect of MTO on SR Ca^{2+} release channels cannot be completely ruled out. In any case, a ryanodine-like mechanism should rather impair SR Ca^{2+} load and hence contraction.

5.3.3 Role of contractile myofilaments

During the last decade, drugs have been discovered which increase force of contraction by an increase in the Ca^{2+} sensitivity of the myofibrillar proteins rather than by elevation of

intracellular Ca^{2+}concentration. Many of these Ca^{2+} sensitizing drugs are characterized by a positive inotropic effect associated with an increase in time course of contraction and a reduction in the amplitude of the Ca^{2+} transient (Blinks and Endoh, 1986; Lee and Allen, 1991; White et al., 1993). In a recent study utilizing rat skinned cardiac fibers, doxorubicin and other anthracyclines were shown to increase tension by direct interaction with the force generating filaments (Bottone et al., 1997). In contrast, no direct effect of doxorubicin on the Ca^{2+} sensitivity of the myofilaments could be demonstrated in membrane-permeabilized cardiac fibers of rabbit (Boucek et al., 1997).

When MTO was applied to fura-2 loaded and current-clamped myocytes, a small but significant rise (10%) of the peak Ca^{2+} transient was observed after 30 min. This rise in intracellular Ca^{2+}concentration must have been due to APD prolongation, because MTO-naive myocytes, when AP-clamped with the same prolonged APD that was recorded before in a current-clamped cell, showed a similar extent of increase of peak Ca^{2+} transients. However, when MTO was applied to cells that were AP-clamped with a constant APD, a decrease instead of an increase of the peak Ca^{2+} transient was observed. Since Ca^{2+} transients in control cells which were not treated with MTO showed a similar decrease within 30 min, MTO has probably no effect on Ca^{2+} transients under this condition. Although promotion of contraction with no increase in the Ca^{2+} transient is compatible with a direct action of MTO on the myofibrillar proteins, a decrease of the transient is expected to result from an increase of the Ca^{2+} affinity of the troponin C (Blinks and Endoh 1986; Lee and Allen, 1991). Whatever the exact mechanisms of MTO's action on the contractile system, it should be noted that some Ca^{2+} sensitizers have also been shown to increase force of contraction without a significant change of the peak Ca^{2+} transient (Ventura et al., 1992; Solaro et al., 1993; Wolska et al., 1996). Finally, long incubations of papillary muscles (> 4 h) with MTO resulted in an increase in resting force, an effect that typically occurs at high concentrations of drugs that increase the myofilament responsiveness to Ca^{2+} (Ferroni et al., 1991; Lee and Allen, 1991; Ventura et al., 1992; Solaro et al., 1993).

Taken together, the results indicate that MTO increases force of contraction in cardiomyocytes via prolongation of APD and by a direct interaction with the contractile system.

5. 4 Clinical relevance

Although the cardiac effects of MTO observed in animal experiments can not be simply extrapolated to the MTO-associated cardiotoxicity demonstrated clinically, some of the findings in this study may have potential clinical relevance.

Cardiac tachyarrhythmias have been observed in patients during MTO therapy (Gams and Wesler, 1984; Posner et al., 1985). Until now, no explanation for these electrocardiographic changes has been presented. The APD-prolonging effect of MTO demonstrated in the present study could be one of the mechanisms underlying MTO-induced arrhythmias. It is well known that prolongation of APD induced by I_{Kr} blockers can be both antiarrhythmic and proarrhythmic, depending on the clinical situation (Sanguinetti and Salata, 1996). APD prolongation is an effective mechanism against reentry-based arrhythmia. On the other hand, excessive lengthening of APD can result in the triggering of early afterdepolarization, one probable mechanism of *torsades de points* arrhythmias. Therefore, it is not unreasonable to speculate that the MTO-induced early afterdepolarization observed in guinea-pig ventricular myocytes may also occur in patients receiving MTO treatment, especially under the conditions which facilitate the APD-prolonging action of MTO, such as sinus bradycardia, hypokalemia and hypomagnesemia.

Reduced ventricular contractile function is a well-documented cardiotoxic effect during chronic MTO therapy (Shenkenberg and von Hoff, 1986; Henderson et al., 1989; Wiseman and Spencer, 1997). In contrast, an increase in contraction of guinea-pig ventricular myocardium in the presence of MTO was observed in this study. Although this acute positive inotropic effect seems to be irrelevant to the myocardial dysfunction induced by MTO, it should be noted that unnecessary enhancement of the contraction force is a waste of energy for the normal heart. In the case of myocardial ischemia, excessive stimulation of the heart could even be harmful. Since cardiac infarction has been reported in patients during MTO therapy (Clark et al., 1984; Gams and Wesler, 1984), special care should be taken when MTO is used for patients with the preexisting cardiac ischemia. Moreover, the pronounced lengthening of relaxation time and increase in resting tension could be detrimental to the heart by impairing ventricular filling. On the other hand, the observation that MTO did not show doxorubicin-like effects on SR function may explain in part its less severe cardiotoxicity compared with that of doxorubicin.

Summary

Mitoxantrone (MTO) is a synthetic anticancer drug derived from anthracendion. The clinical use of MTO is limited by its cardiotoxic effects. Until now, the exact mechanisms of the cardiotoxicity of MTO is still unclear. In an attempt to understand the cellular processes associated with MTO cardiotoxicity, the effects of MTO on the electrical and contractile properties, membrane muscarinic receptors and intracellular calcium concentration in isolated cardiac preparations were investigated in the present study.

In both the isolated guinea-pig papillary muscles and ventricular myocytes, 30 µM MTO induced a time-dependent prolongation of action potential duration (APD) which was occasionally accompanied by early afterdepolarizations. The APD prolonging effect of MTO displayed reverse rate-dependence and was preserved in the presence of 10 µM tetrodotoxin, a specific Na^+ channel blocker.

Under the whole-cell voltage clamp, both the inward rectifier K^+ current (I_{K1}) and the delayed rectifier K^+ current (I_K) of guinea-pig ventricular myocytes were significantly depressed by 30 µM MTO. The rapidly activating component of I_K (I_{Kr}) seemed to be preferentially blocked by MTO. The transient outward current (I_{to}) in rat ventricular myocytes was not affected by MTO.

30 µM MTO had no direct effect on the L-type Ca^{2+} current ($I_{Ca(L)}$), but reversed the inhibitory effect of 1 µM carbamylcholine but not of the A_1-adenosine receptor agonist (-)-N^6-phenylisopropyladenosine (1 µM) on $I_{Ca(L)}$ enhanced by 50 nM isoproterenol in guinea-pig ventricular myocytes. In guinea-pig atrial myocytes, 30 µM MTO inhibited by 93% the muscarinic receptor gated K^+ current ($I_{K,ACh}$) evoked by 1 µM carbamylcholine, whereas $I_{K,ACh}$ elicited by 100 µM GTPγS, a nonhydrolyzable GTP analogue, was only decreased by 12%. The specific binding of [^{3}H]QNB, a muscarinic receptor ligand, to human atrial membranes was concentration-dependently displaced by MTO (1-1000 µM).

In right ventricular papillary muscles, 30 µM MTO increased isometric force of contraction in a time-dependent manner. The force of contraction was increased about 3-fold within 4 h. This positive inotropic effect was accompanied by a prolongation of the time to peak force and relaxation time. An elevation of resting tension could be observed when the muscles were treated with MTO for over 4 h.

In isolated ventricular myocytes, 30 µM MTO caused an increase of cell shortening by 77% and a simultaneous prolongation of APD by 19% within 30 min. Peak amplitude of the

intracellular Ca^{2+} transients as measured by a fluorescent Ca^{2+} indicator fura-2 was also increased by 10%. The contribution of APD prolongation to the enhancement of cell shortening induced by MTO was assessed by clamping control myocytes with action potentials of various duration. Prolongation of APD_{90} by 24% led to an increase of cell shortening by 13%. When the cells were clamped by an action potential with constant APD, MTO still caused an increase of cell shortening by 59% within 30 min. No increase of the peak intracellular Ca^{2+} transients, however, were observed under this condition.

It is concluded that MTO (1) directly blocks cardiac muscarinic receptors; (2) prolongs APD by inhibition of I_{K1} and I_{Kr} ; (3) produces a positive inotropic effect by prolonging APD and by increasing the sensitivity of the contractile proteins to calcium; (4) causes an attenuation of cardiac muscle relaxation. The antimuscarinic effect of MTO might induce tachycardia due to the enhancement of sympathetic activity. The pronounced prolongation of APD with the occasionally occurring early afterdepolarizations may underline the clinically observed dysrhythmias in patients during MTO therapy. Although the positive inotropic effect seems to be irrelevant to the cardiotoxicity of MTO, the pronounced lengthening of relaxation time and increase in resting tension could be detrimental to the heart by impairing ventricular filling.

Zusammenfassung

Mitoxantron (MTO) ist ein synthetisches Anthrachinon-Derivat mit ausgeprägter zytostatischer Wirksamkeit. Der therapeutische Einsatz von MTO wird allerdings durch seine kardiotoxischen Wirkungen eingeschränkt, die sich akut in Form von Rhythmusstörungen und in einer später auftretenden Herzinsuffizienz äußern. Bislang sind die Wirkungsmechanismen der Kardiotoxizität von MTO auf zellulärer Ebene noch nicht untersucht worden. In der vorliegenden Arbeit wurden deshalb die akuten Effekte von MTO auf die elektromechanische Kopplung isolierter Herzmuskelzellen mit Hilfe der patch-clamp Technik, des fluoreszierenden Kalzium-Indikators Fura-2 und der Kontraktilitätsmessung untersucht. Außerdem wurde die Wechselwirkung zwischen MTO und kardialen m-Cholinozeptoren durch Radioliganden-Bindungsstudien analysiert. Die Untersuchungen sollen dazu beitragen, die zellulären Mechanismen der kardiotoxischen Wirkungen von MTO besser zu verstehen. Die Versuche wurden hauptsächlich an ventrikulären Kardiomyozyten des Meerschweinchens durchgeführt.

An isolierten Papillarmuskeln und ventrikulären Kardiomyozyten induzierte MTO (30 µM) eine zeitabhängige Verlängerung der Dauer des Aktionspotentials (APD). Nach einer 3-stündigen Einwirkzeit betrug die Verlängerung der APD an Papillarmuskeln im Mittel 32%. Die APD-Verlängerung unter MTO zeigte eine umgekehrte Frequenz-Abhängigkeit, d.h., der Ausmaß der APD-Verlängerung nahm mit Erhöhung der Reizfrequenz ab. An Kardiomyozyten führte MTO innerhalb von 60 min zu einer Verlängerung der APD um 60%. Frühe Nachdepolarisationen konnten an einigen Zellen beobachtet werden. Vorbehandlung der Kardiomyozyten mit 10 µM Tetrodotoxin, einem spezifischen Na^+-Kanal-Blocker, hatte keinen Einfluß auf die APD-verlängernde Wirkung von MTO. Die Experimente mit Tetrodotoxin zeigen, daß ein residueller Na^+-Einwärtstrom für die APD-Verlängerung nicht verantwortlich war.

Um die APD-verlängernde Wirkung von MTO aufzuklären, wurde der Einfluß von MTO auf Kaliumauswärtsströme untersucht. An ventrikulären Kardiomyozyten wurde sowohl der einwärts gleichrichtende K^+-Strom (I_{K1}) als auch der verzögert gleichrichtende K^+-Strom (I_K) durch 30 µM MTO innerhalb von 60 min um ca. 50% gehemmt. Experimente, in denen die schnell aktivierende Komponente von I_K (I_{Kr}) direkt gemessen wurde, zeigten, daß der Effekt von MTO I_{Kr}-spezifisch war. Der transiente K^+-Auswärtstrom (I_{to}) ventrikulärer Kardiomyozyten der Ratte wurde durch MTO nicht beeinflußt. Diese Experimente wurde an

der Ratte durchgeführt, da an dieser Spezies wie auch am Mensch diese K^+-Stromkomponente nachweisbar ist. Meerschweinchen zeigt kein I_{to}. MTO hatte auch keine direkte Wirkung auf den spannungsabhängigen Kalziumeinwärtsstrom (I_{Ca}).

Sowohl funktionelle Experimente an Acetylcholin-induziertem K^+-Strom ($I_{K,ACh}$) an Vorhofzellen als auch Radioliganden-Bindungsstudien mit [^{3}H]-QNB an menschlichen Vorhofmembranen zeigten, daß MTO ein Antagonist an kardialen m-Cholinozeptoren ist, d.h. atropinartige Wirkung besitzt.

An isometrisch sich kontrahierenden Papillarmuskeln konnte für MTO überraschenderweise eine konzentrationsabhängige positiv inotrope Wirkung nachgewiesen werden, die sich langsam über mehreren Stunden entwickelte. Die Kontraktionskraft wurde durch 30 µM MTO innerhalb von 4 Stunden um das fast 3-fache verstärkt. Parallel zur inotropen Wirkung kam es zu einer signifikanten Verlängerung der Gesamtkontraktionsdauer, ein Effekt, der sowohl auf eine Verlängerung der Anstiegszeit (um 31%) als auch der Erschlaffungszeit (um 47%) zurückzuführen war. Wurden die Muskeln länger als 4 Stunden mit 30 µM MTO behandelt, entwickelte sich häufig im Anschluß an die positiv inotrope Wirkung eine Kontraktur (Erhöhung der muskulären Ruhespannung), die von einer Abnahme des Kontraktionsmaximums begleitet war.

An isotonisch sich verkürzenden ventrikulären Myozyten führte 30 µM MTO innerhalb von 30 min zu einer Verstärkung der Zellverkürzung um 77%. Gleichzeitig wurde die APD um 19% verlängert, und die Amplitude des intrazellulären Ca^{2+}-Transienten um 10% erhöht. Um herauszufinden, in welchem Ausmaß die Verlängerung des Aktionspotentials zur positiv inotropen Wirkung von MTO beiträgt, wurden die Myozyten durch Aktionspotentiale unterschiedlicher Dauer stimuliert, und die dadurch induzierte Zellverkürzung gemessen. Es zeigte sich, daß eine Verlängerung der APD um 24% nur zu einer Verstärkung der Zellverkürzung um 13% führte. Wurden die Myozyten durch ein Aktionspotential konstanter Dauer stimuliert, zeigte MTO immer noch einen positiv inotropen Effekt, die Zellverkürzung nahm innerhalb von 30 min um 59% zu, während der intrazelluläre Ca^{2+}-Transienten unbeeinflußt blieb. Diese Befunde zeigen, daß die Verstärkung der Kontraktion in Anwesenheit von MTO nur teilweise auf einer Verlängerung der APD beruht. Ein wesentlicher Teil der positiv inotropen Wirkung ist demnach auf eine direkte Wechselwirkung zwischen MTO und den kontraktilen Proteinen der Herzmuskelzelle zurückzuführen.

Zusammenfassend läßt sich sagen, daß MTO folgende Wirkungen auf Herzmuskelzellen besitzt: (1) Blockade von m-Cholinozeptoren; (2) Verlängerung des Aktionspotentials als

Folge einer Hemmung von I_{K1} und I_{Kr}; (3) Verstärkung der Muskelkontraktion als Resultat der Verlängerung der APD und einer erhöhten Kalziumempfindlichkeit der kontraktilen Proteine; (4) Verzögerung der Muskelrelaxation. Einige der Effekte könnten für die in der Klinik beobachtete kardiotoxische Wirkungen verantwortlich sein. Die atropinartige Wirkung von MTO könnte zu tachykarden Episoden führen. Frühe Nachdepolarisationen als Folge der APD-Verlängerung sind möglicherweise Ursprung für die unter MTO-Behandlung immer wieder beobachteten Arrhythmien. Ferner würde eine Verlängerung der Kontraktionsdauer und die Manifestation einer Kontraktur zu einer deutlichen Beeinträchtigung der Ventrikelfunktion führen.

6. References

Abramson JJ, Buck E, Salama G, Casida JE and Pessah IN (1988) Mechanism of anthraquinone-induced calcium release from skeletal muscle sarcoplasmic reticulum. *J Biol Chem* **263:**18750-18758.

Alderton PM, Gross J and Green MD (1992). Comparative study of doxorubicin, mitoxantrone, and epirubicin in combination with ICRF-187 (ADR-529) in chronic cardiotoxicity animal model. *Cancer Res* **52:**194-201.

Arnaiz and Llesuy (1993). Oxidative stress in mouse heart by antitumoral drugs: a comparative study of doxorubicin and mitoxantrone. *Toxicology* **77:**31-38.

Attwell D, Cohen I and Eisener D (1981). The effects of heart rate on the action potential of guinea-pig and human ventricular muscle. *J Physiol (London)* **313:**439-461.

Backx PH and Marban E (1993). Background potassium current active during the plateau of the action potential in guinea pig ventricular myocytes. *Circ Res* **72:**890-900.

Bassani JW, Bassani RA and Bers DM (1994). Relaxation in rabbit and rat cardiac cells: species-dependent differences in cellular mechanisms. *J Physiol (London)* **476:**279-293.

Belardinelli L, Linden J and Berne RM (1989). The cardiac effects of adenosine. *Prog Cardiovasc Dis* **32:**73-97.

Benjamin RS (1995). Rationale for the use of mitoxantrone in the older patient: cardiac toxicity. *Semin Oncol* **22:**11-13.

Bers DM (1991). Control of cardiac contraction by SR Ca release and sarcolemmal Ca fluxes. In: Bers DM, ed. *Excitation-Contraction Coupling and Cardiac Contractile Force.* Norwell, Mass: Kluwer Academic Publishers; pp.149-170.

Bers DM and Bridge JHB (1989). Relaxation of rabbit ventricular muscle by Na-Ca exchange and sarcoplasmic reticulum Ca-pump: ryanodine and voltage sensitivity. *Circ Res* **65:**334-342.

Bers DM, Lederer WJ and Berlin JR (1990). Intracellular Ca transients in rat cardiac myocytes: role of Na-Ca exchange in excitation-contraction coupling. *Am J Physiol* **258:**C944-C954.

Blinks JR and Endoh M (1986). Modification of myofibrillar responsiveness to Ca^{++} as an inotropic mechanism. *Circulation* **73:**III85-III98.

Blum RH and Carter SK (1974). Adriamycin: a new anticancer drug with significant clinical activity. *Ann Intern Med* **80:**249-259.

Bosch RF, Gaspo R, Busch AE, Lang H-J, LI GR and Nattel S (1997). Effects on repolarization of the chromanol 293B, a highly selective blocker of the slow component of the delayed rectifier K^+ current (I_{Ks}) in human and guinea pig ventricle. *J Am Coll Cardiol* **29:**512A (abstract).

Bottone AE, de Beer EL and Voest EE (1997). Anthracyclines enhance tension development in cardiac muscle by direct interaction with the contractile system. *J Mol Cell Cardiol* **29:**1001-1008.

Boucek RJ, Dodd DA, Atkinson JB, Oquist N and Olson RD (1997). Contractile failure in chronic doxorubicin-induced cardiomyopathy. *J Mol Cell Cardiol* **29:**2631-2640.

Bradford MM (1976). A rapid and sensitive method for quantification of microgram quantities of protein utilizing the principle of protein-dye binding. *Anal Biochem* **42:**248-254.

Breitwieser GE and Szabo G. (1985). Uncoupling of cardiac muscarinic and ß-adrenergic receptors from ion channels by a guanine nucleotide analogue. *Nature (London)* **317:**538-540.

Bridge JHB, Spitzer KW and Ershler PR (1988). Relaxation of isolated ventricular cardiomyocytes by a voltage-dependent process. *Science* **241:**823-825.

Brixius K, Pietsch M, Hoeschen S, Muller-Ehmsen J and Schwinger RH (1997). Effect of inotropic interventions on contraction and Ca^{2+} transients in the human heart. *J Appl Physiol* **83:**652-660.

Buggisch D, Isenberg G, Ravens U and Scholtysik G (1985). The role of sodium channels in the effects of the cardiotonic compound DPI 201-106 on contractility and membrane potentials in isolated mammalian heart preparations. *Eur J Pharmacol* **118:**303- 311.

Busch AE, Suessbrich H, Waldegger S, Sailer E, Greger R, Lang H, Lang F, Gibson KJ and Maylie JG (1996). Inhibition of I_{Ks} in guinea pig cardiac myocytes and guinea pig I_{sK} channels by the chromanol 293B. *Pfluegers Arch* **432:**1094-1096.

Clark GM, Tokaz LK, von Hoff DD, Thoi LL and Coltman CA (1984). Cardiotoxicity in patients treated with mitoxantrone on southwest oncology group phase II protocols. *Cancer Treat Symp* **3:**25-30.

Dodd DA, Atkinson JB, Olson RD, Buck S, Cusack BJ, Fleischer S and Boucek RJ (1993). Doxorubicin cardiomyopathy is associated with a decrease in calcium release channel of the sarcoplasmic reticulum in a chronic rabbit model. *J Clin Invest* **91:**1697-1705.

Doroshow JH (1983). Anthracycline antibiotic-stimulated superoxide, hydrogen peroxide, and hydroxyl radical production by NADH dehydrogenase. *Cancer Res* **43:**4543-4551.

Doroshow JH and Davies KJ (1983). Comparative cardiac oxygen radical metabolism by anthracycline antibiotics, mitoxantrone, bisantrene, 4'-(9-acridinylamino)-methanesulfon-m-anisidide, and neocarzinostation. *Biochem Pharmacol* **32:**2935-2939.

Dorr RT. Cytoprotective agents for anthracyclines (1996). *Semin Oncol* **23 (Suppl. 8):**23-34.

Dukes ID and Morad M (1991). The transient K^+ current in rat ventricular myocytes: evaluation of its Ca^{2+} and Na^+ dependence. *J Physiol (London)* **435:**395-420.

Fabiato A (1985). Simulated calcium current can both cause calcium loading in and trigger calcium release from the sarcoplasmic reticulum of a skinned canine cardiac Purkinje cell. *J Gen Physiol* **85:**291-320.

Faulds D, Balfour JA, Chrisp P and Langtry HD (1991). Mitoxantrone: a review of its pharmacodynamic and pharmacokinetic properties, and therapeutic potential in the chemotherapy of cancer. *Drugs* **41:**400-449.

Ferroni C, Hano O, Ventura C, Lakatta EG, Klockow M, Spurgeon H and Capogrossi MC (1991). A novel positive inotropic substance enhances contractility without increasing the Ca^{2+} transient in rat myocardium. *J Mol Cell Cardiol* **23:**325-331.

Gams RA and Wesler MJ (1984). Mitoxantrone cardiotoxicity: results from southeastern cancer study group. *Cancer Treat Symp* **3:**31-33.

Ganitkevich VYa and Isenberg G (1991). Depolarization-mediated intracellular calcium transients in isolated smooth muscle cells of guinea-pig urinary bladder. *J Physiol (London)* **435:**182-205.

Gjini V, Korth M, Schreieck J, Weyerbrock S, Schömig A. and Schimitt C (1996). Differential class III antiarrhythmic effects of ambasilide and dofetilide at different extracellular potassium and pacing frequencies. *J Cardiovasc Pharmacol* **28:**314-320.

Grynkiewicz G, Poenie M and Tsien RY (1985). A new generation of Ca^{2+} indicators with greatly improved fluorescence properties. *J Biol Chem* **260:**3440-3450.

Gwilt M, Arrowsmith JE, Blackburn KJ, Burges RA, Cross PE, Dalrymple HW and Higgins AJ (1991). UK-68,798: A novel, potent and highly selective class III antiarrhythmic agent which blocks potassium channels in cardiac cells. *J Pharmacol Exp Ther* **256:**318-324.

Hajjar RJ, Schmidt U, Helm P and Gwathmey JK (1997). Ca^{++} sensitizers impair cardiac relaxation in failing human myocardium. *J Pharmacol Exp Ther* **280:**247-254.

Halili-Rutman I, Hershko C, Link G, Rutman AJ and Shainberg A (1997). Inhibition of calcium accumulation by the sarcoplasmic reticulum: a putative mechanism for the cardiotoxicity of adriamycin. *Biochem Pharmacol* **54:**211-214.

Hamill OP, Marty A, Neher E, Sakmann B and Sigworth FJ (1981). Improved patch-clamp techniques for high-resolution current recording from cells and cell-free membrane patches. *Pfluegers Arch* **391:**85-100.

Heath BM and Terrar DA (1996). Separation of the components of the delayed rectifier potassium current using selective blockers of I_{Kr} and I_{Ks} in guinea-pig isolated ventricular myocytes. *Exp Physiol* **81:**587-603.

Henderson BM, Dougherty WJ, James VC, Tilly LP and Noble JF (1982). Safety assessment of a new anticancer compound, mitoxantrone, in beagle dogs: comparison with doxorubicin. I. clinical observations. *Cancer Treat Rep* **66:**1139-1143.

Henderson IC, Allegra JC, Woodcock T, Wolff S, Bryan S, Cartwright K, Dukart G and Henry D (1989). Randomized clinical trial comparing mitoxantrone with doxorubicin in previously treated patients with metastatic breast cancer. *J Clin Oncol* **7:**560-571.

Herman EH, Ferrans VJ, Myers CE and von Vleet JF (1985). Comparison of the effectiveness of (±)-1,2-bis(2,5-deoxopiperanizyl-1-yl)-propane (ICRF-187) and N-acetylcysteine in preventing chronic doxorubicin cardiotoxicity in beagles. *Cancer Res* **45:**246-281.

Herman EH, Zhang J, Hasinoff BB, Clark JR and Ferrans VJ (1997). Comparison of the structural changes induced by doxorubicin and mitoxantrone in the heart, kidney and intestine and characterization of the Fe(III)-mitoxantrone complex. *J Moll Cell Cardiol* **29:**2415-2430.

Hiraoka M, Furukawa T, Sawanobort T and Yamane T (1995). Regulation of delayed rectifier K^+ channels and ATP-sensitive K^+ channels by intracellular factors. In: Vereecke J, van Bogaert P and Verdonck F, ed. *Potassium channels in normal and pathological conditions*. Leuven: Leuven University Press; pp.103-117.

Holmberg SRM and Williams AJ (1990). Patterns of interaction between anthraquinone drugs and the calcium-release channel from cardiac sarcoplasmic reticulum. *Circ Res* **67:**272-283.

Hondeghem L and Snyders D (1990). Class III antiarrhythmic agents have a lot of potential but a long way to go: reduced effectiveness and dangers of reverse use dependence. *Circulation* **81:**686-690.

Honerjäger P (1982). Cardioactive substances that prolong the open state of sodium channels. *Rev Physiol Biochem Pharmacol* **92:**1-74.

Horn R and Marty A (1988). Muscarinic activation of ionic currents measured by a new whole-cell recording method. *J Gen Physol* **92:**145-159.

Jensen RA. Doxorubicin cardiotoxicity: contractile changes after long term treatment in the rat (1986). *J Pharmacol Exp Ther* **236:**197-203.

Johnson RK, Zee-Cheng RK-Y, Lee WW, Acton EM, Henry DW and Cheng CC (1979). Experimental antitumor activity of aminoanthraquinones. *Cancer Treat Rep* **63:**425-439.

Josephson IR, Sanchez-chapula J and Brown AM (1984). Early outward current in rat single ventricular cells. *Circ Res* **54:**157-162.

Jurkiewicz NK and Sanguinetti MC (1993). Rate-dependent prolongation of cardiac action potentials by a methanesulfonanilide class III antiarrhythmic agent. Specific block of rapidly activating delayed rectifier K^+ current by dofetilide. *Circ Res* **72:**75-83.

Jurkiewicz NK, Wang J, Fermini B, Sanguinetti MC and Salata JJ (1996). Mechanism of action potential prolongation by RP 58866 and its active enantiomer, terikalant. Block of the rapidly activating delayed rectifier K^+ current, I_{kr}. *Circulation* **94:**2938-2946.

Kantrowitz NE and Bristow MR (1984). Cardiotoxicity of antitumor agents. *Prog Cardiovasc Dis* **27:**195-200.

Katritsis D and Camm AJ (1993). New class III antiarrhythmic drugs. *Eur Heart J* **14:**93-99.

Kharasch ED and Novak RF (1983). Inhibitory effects of anthracenedione antineoplastic agents on hepatic and cardiac lipid peroxidation. *J Pharmacol Exp Ther* **226:**500-506.

Kharasch ED and Novak RF (1985). Mitoxantrone and ametantrone inhibit hydroperoxide-dependent initiation and propagation reactions in fatty acid peroxidation. *J Biol Chem* **260:**10645-10652.

Kim DH, Landry AB, Lee YS and Katz AM (1989). Doxorubicin-induced calcium release from cardiac sarcoplasmic reticulum vesicles. *J Mol Cell Cardiol* **21:**433-436.

Kim E, Giri SN and Pessah IN (1994). Antithetical actions of mitoxantrone and doxorubicin on ryanodine-sensitive Ca^{++} release channels of rat cardiac sarcoplasmic reticulum: evidence for a competitive mechanism. *J Pharmacol Exp Ther* **268:**1212-1221.

Kiyosue T and Arita M (1989). Late sodium current and its contribution to action potential configuration in guinea pig ventricular myocytes. *Circ Res* **64:**389-397.

Kurachi Y, Nakajima T and Sugimoto T (1986). On the mechanism of activation of muscarinic K^+ channels by adenosine in isolated atrial cells: involvement of GTP-binding proteins. *Pfluegers Arch* **407:**264-274.

Kurachi Y, Nakajima T and Sugimoto T (1987). Short-term desensitisation of muscarinic K^+ channel current in isolated atrial myocytes and possible role of GTP-binding proteins. *Pfluegers Arch* **410:**227-233.

Lee JA and Allen DG (1991). EMD 53998 sensitizes the contractile proteins to calcium in intact ferret ventricular muscle. *Circ Res* **69:**927-936.

Lefrak EA, Pitha J, Rosenheim S and Gottlieb JA (1973). A clinicopathologic analysis of adriamycin cardiotoxicity. *Cancer* **32:**302-314.

Legha SS, Wang YM, Mackay B, Ewer M, Hortobagy GN, Benjamen SR and Ali MK (1982). Clinical and pharmacologic investigation of the effects of α-tocopherol on adramycin cardiotoxicity. *Ann N Y Acad Sci* **393:**411-418.

Lewartowski B, Hansford RG, Langer GA and Lakatta EG (1990). Contraction and sarcoplasmic reticulum Ca^{2+} content in single myocytes of guinea pig heart: effect of ryanodine. *Am J Physiol* **259:**H1222-H1229.

Malonne H and Atassi G (1997). DNA topoisomerase targeting drugs: mechanisms of action and perspectives. *Anticancer Drugs* **8:**811-822.

Minotti G (1993). Sources and role of iron in lipid peroxidation. *Chem Res Toxicol* **6:**134-146.

Minotti G, Gairo G and Monti E (1999). Role of iron in anthracycline cardiotoxicity: new tunes for an old song? *FASEB J* **13:**199-212.

Morad M and Trautwein W (1968). The effect of the duration of the action potential on contraction in the mammalian heart tissue. *Pfluegers Arch* **299:**66-82.

Murdock KC, Child RG, Fabio PF, Angier RB, Wallace RE, Durr FE and Citarella RV. Antitumor agents (1979). I. 1,4-bis[(aminoalkyl)amino]-9,10-anthracenediones. *J Med Chem* **22:**1024-1030.

Myers C, Bonow R, Palmieri S, Jenkins J Carden B, Locker G, Doroshow J and Epstein SA (1983). A randomized controlled trial assessing the prevention of doxorubicin cardiomyopathy by N-acetylcysteine. *Semin Oncol* **10 (Suppl):**53-55.

Myers CE, Gianni L, Zweier J, Muinde J, Sinha BK and Eliot H (1986). Role of iron in adriamycin biochemistry. *Fed Proc* **45:**2792-2797.

Nagasaki K and Fleischer S (1989). Modulation of the calcium release channel of sarcoplasmic reticulum by adriamycin and other drugs. *Cell Calcium* **10:**63-70.

Narahashi T (1974) Chemicals as tools in the study of excitable membranes. *Physiol Rev* **54:**813-889.

Neidhart JA, Gochnour D, Roach R, Hoth D and Young D (1986). A comparison of mitoxantrone and doxorubicin in breast cancer. *J Clin Oncol* **4:**672-677.

Olson HM, Young DM, Prieur DJ, LeRoy AF and Reagan RL (1974). Electrolyte and morphological alterations of myocardium in adriamycin-treated rabbits. *Am J Pathol* **77:**439-454.

Olson RD, Boerth RC, Gerber JG and Nies AS (1981). Mechanism of adriamycin cardiotoxicity: evidence for oxidative stress. *Life Sci* **29:**1393-1401.

Olson RD and Mushlin PS (1990). Doxorubicin cardiotoxicity: analysis of prevailing hypotheses. *FASEB J* **4:**3076-3086.

Ondrias K, Borgatta L, Kim DH and Ehrlich BE (1990). Biphasic effects of doxorubicin on the calcium release channel from sarcoplasmic reticulum of cardiac muscle. *Circ Res* **67:**1167-1174.

Perkins WE, Schroeder RL, Carrano RA and Imondi AR (1984). Myocardial effects of mitoxantrone and doxorubicin in the mouse and guinea pig. *Cancer Treat Rep* **68:**841-847.

Pessah IN, Durie EL, Schiedt MJ and Zimanyi I (1990). Anthraquinone-sensitized Ca^{2+} release Channel from rat cardiac sarcoplasmic reticulum: possible receptor-mediated mechanism of doxorubicin cardiomyopathy. *Mol Pharmacol* **37:**503-514.

Pessah IN, Schiedt MJ, Shalaby MA, Mack M and Giri SN (1992). Etiology of sarcoplasmic reticulum calcium release channel lesions in doxorubicin-induced cardiomyopathy. *Toxicology* **72:**189-206.

Pfaffinger PJ, Martin JM, Hunter DD, Nathanson NM and Hille B (1985). GTP-binding proteins couple cardiac muscarinic receptors to a K channel. *Nature (London)* **317:**536-538.

Posner LE, Dukart G, Goldberg J, Bernstein GT and Cartwright K (1985). Mitoxantrone: an overview of safety and toxicity. *Invest New Drugs* **3:**123-132.

Powell T, Terrar DA and Twist VW (1980). Electrical properties of individual cells isolated from adult rat ventricular myocardium. *J Physiol (London)* **302:**131-153.

Powis G (1989). Free radical formation by antitumor quinones. *Free Radical Biol Med* **6:**63-101.

Rabkin SW (1983). Interaction of external calcium concentration and verapamil on the effects of doxorubicin (Adriamycin) in the isolated heart preparation. *J Cardiovasc Pharmacol* **5:**848-855.

Raffaeli S, Ferroni C, Spurgeon HA and Capogrossi MC (1989). Milrinone enhances cytosolic calcium transient and contraction in rat cardiac myocytes during beta-adrenergic stimulation. *Int J Cardiol* **25:**S63-S69.

Reiter M (1972). Differences in the inotropic cardiac effects of noradrenaline and dihydro-ouabain. *Naunyn-Schmiedeberg's Arch Pharmacol* **275:**243-250.

Revis N and Marusic N (1979). Effects of doxorubicin and its aglycone metabolite on calcium sequestration by rabbit heart, liver, and kidney mitochondria. *Life Sci* **25:**1055-1064.

Rhoden W, Hasleton P and Brooks N (1993). Anthracyclines and the heart. *Br Heart J* **70:**499-502.

Ryan TP and Aust SD (1992). The role of iron in oxygen-mediated toxicities. *Crit Rev Toxicol* **22:**119-141.

Salata JJ, Jurkiewicz NK, Sanguinetti MC, Siegl PK, Claremon DA, Remy DC, Elliot JM and Libby BE (1996). The novel class III antiarrhythmic agent, L-735,821 is a potent and selective blocker of I_{Ks} in guinea pig ventricular myocytes. *Circulation* **94:**I-529 (abstract).

Sanguinetti MC and Jurkiewicz NK (1990a). Two components of cardiac delayed rectifier K^+ current: differential sensitivity to block by class III antiarrhythmic agents. *J Gen Physiol* **96:**195-215.

Sanguinetti MC and Jurkiewicz NK (1990b). Lanthanum blocks a specific component of I_K and screens membrane surface charge in cardiac cells. *Am J Physiol* **259:**H1881-H1889.

Sanguinetti MC and Salata JJ (1996). Cardiac potassium channel modulators: potential for antiarrhythmic therapy. In: Evans JM, Hamilton TC, Longman SD and Stemp G, ed. *Potassium channels and their modulators.* London: Taylor and Francis Ltd; pp. 221-256.

Sakakibara Y, Rurukawa T, Singer DH, Jia H, Backer CL, Arentzen CE and Wsserstrom JA (1993). Sodium current in isolated human ventricular myocytes. *Am J Physiol* **265:**H1301-H1309.

Schreieck J, Wang Y, Gjini V, Korth M, Zrenner B, Schömig A. and Schimitt C. (1997). Differential effect of ß-adrenergic stimulation on the frequency-dependent electrophysiologic actions of the new class III antiarrhythmics dofetilide, ambasilide and chromanol 293B. *J Cardiovasc Electrophysiol* **8:**1420-1430.

Shenkenberg TD and von Hoff DD (1986). Mitoxantrone: a new anticancer drug with significant clinical activity. *Ann Intern Med* **105:**67-81.

Shibasaki T (1987). Conductance and kinetics of delayed rectifier potassium channels in nodal cells of the rabbit heart. *J Physiol (London)* **387:**227-250.

Shimoni Y, Clark RB and Giles WR (1992). Role of inwardly rectifying potassium current in rabbit ventricular action potential. *J Physiol (London)* **448:**709-728.

Shipp NG, Dorr RT, Alberts DS, Dawson BV and Hendrix M (1993). Characterization of experimental mitoxantrone cardiotoxicity and its partial inhibition by ICRF-187 in cultured neonatal rat heart cells. *Cancer Res* **53:**550-556.

Singal PK, Forbes MS and Sperelakis N. Occurrence of intramitochondrial Ca^{++} granules in a hypertrophied heart exposed to adriamycin (1983). *Can J Physiol Pharmacol* **62:**1239-1244.

Singal PK and Iliskovic N (1998). Doxorubicin-induced cardiomyopathy. *N Engl J Med* **339:**901-905.

Singal PK, Iliskovic N, Li T and Kumar D (1997). Adrimycin cardiomyopathy: pathophysiology and prevention. *FASEB J* **11:**931-936.

Sparano BM, Gordon G, Hall C, Iatropoulos MJ and Noble JF (1982). Safety assessment of a new anticancer compound, mitoxantrone, in beagle dogs: comparison with doxorubicin. II. histologic and ultrastructural pathology. *Cancer Treat Rep* **66:**1145-1158.

Spector PS, Curran ME, Zou A, Keating MT and Sanguinetti MC (1996). Fast inactivation causes rectification of the I_{Kr} channel. *J Gen Physiol* **107:**611-619.

Shenkenberg TD and von Hoff DD (1986). Mitoxantrone: a new anticancer drug with significant clinical activity. *Ann Intern Med* **105:**67-81.

Solaro RJ, Gambassi G, Warshaw DM, Keller MR, Spurgeon HA, Beier N and Lakatta EG (1993). Stereoselective actions of thiadiazinones on canine cardiac myocytes and myofilaments. *Circ Res* **73:**981-990.

Speyer JL, Green MD, Kramer E, Rey M, Sanger JA, Wernz J, Feit F, Slater W, Blum R and Muggia M (1988). Protective effect of the bispiperazine ICRF-187 against doxorubicin induced cardiac toxicity in women with advanced breast cancer. *N Engl J Med* **319:**745-752.

Steinberg JS, Cohen AJ, Wasserman AG, Cohen P and Ross AM (1987). Acute arrhythmogenicity of doxorubicin administration. *Cancer* **60:**1213-1218.

Tande PM, Bjornstad H, Yang T and Refsum H (1990). Rate-dependent class III antiarrhythmic action, negative chronotropy, and positive inotropy of a novel I_K blocking drug, UK-68,798: potent in guinea pig but no effect in rat myocardium. *J Cardiovasc Pharmacol* **16:**401-410.

Terrar DA and White E (1989). Mechanism of potentiation of contraction by depolarization during action potentials in guinea-pig ventricular muscle. *Q J Exp Physiol* **74:**355-358.

Tumminello FM, Leto G, Gebbia N, Gebbia V, Russo A and Rausa L (1987). Acute myocardial effects of mitoxantrone in the rabbit. *Cancer Treat Rep* **71:**529-531.

Unverferth DV, Unverferth BJ, Balcerzak SP, Bashore TA and Neidhart JA (1983). Cardiac evaluation of mitoxantrone. *Cancer Treat Rep* **67:**343-350.

Van Vleet JF, Ferrans JV and Weirich WE (1980). Cardiac disease induced by chronic adriamycin administration in dogs and an elevation of vitamin E and selenium and cardioprotectants. *Am J Pathol* **99:**13-22.

Varro A and Papp JG (1995). Classification of positive inotropic actions based on electrophysiologic characteristics: where should calcium sensitizers be placed? *J Cardiovasc Pharmacol* **26**:S32-S44.

Ventura C, Miller R, Wolf HP, Beier N, Jonas R, Klockow M, Lues I, Hano O, Spurgeon HA, Lakatta EG and Capogrossi MC (1992). Novel diazinone derivatives separate myofilament Ca^{2+} sensitization and phosphodiesterase III inhibitory effects in guinea pig myocardium. *Circ Res* **70:**1081-1090.

Von Hoff DD, Rozencweig M, Layard M, Slavic M and Muggia FM (1977). Daunomycin-induced cardiotoxicity in children and adults: a review of 110 cases. *Am J Med* **62:**200-208.

Von Hoff DD, Layard MW, Basa P, Davis HL, von Hoff AL, Rozencweig M and Muggia FM (1979). Risk factors for doxorubicin-induced congestive heart failure. *Ann Intern Med* **91:**710-717.

Wallace RE, Murdock KC, Angier RB and Durr FE (1979). Activity of a normal anthracenedione, 1,4-dihydrxy-5,8-bis((2-(2-hydroxyethyl)amino))-9,10-anthracenedione dihydrochloride, against experimental tumors in mice. *Cancer Res* **39:**1570-1574.

Wang YX and Korth M (1995). Effects of doxorubicin on excitation-contraction coupling in guinea pig ventricular myocardium. *Circ Res* **76:**645-653.

Weiss RB (1989). Mitoxantrone: its development and role in clinical practice. *Oncology* **3:**135-147.

Wettwer E, Scholtysik G, Schaad A, Himmel H and Ravens U (1991). Effects of the new class III antiarrhythmic drug E-4031 on myocardial contractility and electrophysiological parameters. *J Cardiovasc Pharmacol* **17:**480-487.

White J, Lee JA, Shah N and Orchard CH (1993). Differential effects of the optical isomers of EMD 53998 on contraction and cytoplasmic Ca^{2+} in isolated ferret cardiac muscle. *Circ Res* **73:**61-70.

Wiseman LR and Spencer CM (1997). Mitoxantrone. A review of its pharmacology and clinical efficacy in the management of hormone-resistant advanced prostate cancer. *Drugs and Aging* **10:**473-485.

Wolska BM, Kitada Y, Palmiter KA, Westfall MV, Johnson MD and Solaro RJ (1996). CGP-48506 increases contractility of ventricular myocytes and myofilaments by effects on actin-myosin reaction. *Am J Physiol* **270:**H24-H32.

Wortman JE, Lucas VS, Schuster E, Thiele D and Logue GL (1979). Sudden death during doxorubicin administration. *Cancer* **44:**1588-1591.

Yamada M, Inanobe A and Kurachi Y (1998). G protein regulation of potassium ion channels. *Pharmacol Rev* **50:**723-757.

Yang T and Roden DM (1996). Extracellular potassium modulation of drug block of I_{Kr}: implications for torsades de pointes and reverse use-dependence. *Circulation* **93:**407-411.

Yang T, Snyders DJ and Roden DM (1997). Rapid inactivation determines the rectification and $[K^+]_o$ dependence of the rapid component of the delayed rectifier K^+ current in cardiac cells. *Circ Res* **80:**782-789.

Young RC, Ozols RF and Myers CE (1981). The anthracycline antineoplastic drugs. *N Engl J Med* **305:**139-153.

Zeng J, Laurita KR, Rosenbaum DS and Rudy Y (1995). Two components of the delayed rectifier K current in ventricular myocytes of the guinea pig type: theoretical formulation and their role in repolarization. *Circ Res* **77:**140-152.

Zorzato F, Salviati G, Facchinetti T and Volpe P (1985). Doxorubicin induces calcium release from terminal cisternae of skeletal muscle: A study on isolated sarcoplasmic reticulum and chemically skinned fibers. *J Biol Chem* **260:**7349-7355.

Abbreviations

AMP	adenosine monophosphate
AP-clamp	action potential clamp
APD	action potential duration
APD_{90}	action potential duration measured at 90% of repolarization
ATP	adenosine triphosphate
B_{max}	maximum binding capacity
C_m	membrane capacitance
CCh	carbamylcholine
DMSO	dimethy sulfoxide
EDTA	ethylendiaminetetracetic acid
EGTA	ethylene glycol-bis(ß-aminoethylether)-N,N,N',N'-tetraacetic acid
GTP	guanosine triphosphate
GTP-γS	guanosine-5'-O-(3-thiotriphosphate)
HEPES	N-(2-hydroxyethyl)piperazine-N'-(2-ethanesulfonic acid)
$I_{Ca(L)}$	L-type Ca^{2+} current
I_K	delayed rectifier K^+ current
I_{K1}	inward rectifier K^+ current
$I_{K,ACh}$	muscarinic receptor gated K^+ current
I_{Kr}	rapidly activating delayed rectifier K^+ current
I_{Ks}	slowly activating delayed rectifier K^+ current
I_{to}	transient outward current
ISO	(±)-isoproterenol
MOPS	3-(N-morpholino)butanesulfonic acid
MTO	mitoxantrone
NADH	reduced nicotinamide adenine dinucleotide
QNB	quinuclidinyl benzylate
R-PIA	(-)-N^6-phenylisopropyladenosine
SR	sarcoplasmic reticulum
TEA	tetraethylammonium
TTX	tetrodotoxin

Risk and safety codes of the hazardous chemicals used in this study

Amphotericin B (R: 20/21-36/37/38-40; S: 45-36/37/39)

Atropine (R: 26/27/28-43; S: 45-36/37/39-22)

Carbamylcholine (R: 26/27/28-36/37/38; S: 45-36/37/39-22)

Dimethy sulfoxide (R: 20/21/22-36/37/38-42/43; S: 26-36-23)

Guanosine-5'-O-(3-thiotriphosphate) (R: 36/37/38; S: 26-36)

[^{3}H]-Quinuclidinyl benzylate (R: 23/24/25; S: 22-45-36/37/39)

(±)-Isoproterenol (R: 20/21/22-36/37/38; S: 26-36)

Mitoxantrone (R: 46-61; S: 45-36/37/39)

D-Sotalol (R: 36/37/38; S: 26-36)

Tetrodotoxin (R: 26/27/28; S: 45-36/37/39-22)

Acknowledgements

I am deeply indebted to Prof. M. Korth for his encouragement and guidance of the project.

My special gratitude is extended to Prof. H.J. Duchstein and Prof. D. Gefffken for their generous help and valuable suggestions.

I would like to thank Dr. Xiaobo Zhou for his technical advice and helpful discussions.

Curriculum Vitae

Name:	Gexin Wang
Birthday:	March 28, 1960
Birthplace:	Shanghai, P.R. China
Nationality:	P.R. China
Marital status:	Married, one daughter

Education:

09/1967-07/1973:	Xiangyang Primary School, Shanghai, China
09/1973-07/1978:	Jinggang High School, Shanghai, China
09/1978-07/1982:	School of Pharmacy, Shanghai Medical University Acquired degree: Bachelor of Science
02/1985-07/1985:	Intensive English Course, Shanghai Normal University
09/1986-06/1987:	Germane Course, Shanghai Foreign Language University
10/1988-03/1989:	Advanced Germane Course at Goethe Institute Mannheim, Germany
11/1993-07/1995:	Postgraduate training in Pharmacology, Hunan Medical University Acquired degree: Master of Medicine
04/1997-06/2000:	Doctoral progam at Fachbereich Chemie, Universität Hamburg, Germany

Professional Experience:

10/1982-07/1988:	Assistant of pharmacology at the Shanghai Railway Medical College
04/1989-02/1992:	Research fellow at Institut für Pharmakologie und Toxikologie der Technischen Universität München, Germany (DAAD fellowship)
04/1992-09/1996:	Lecturer of pharmacology at the Medical College, Shanghai Tie-Dao University
10/1996-08/2000:	Research fellow at Abteilung für Pharmakologie für Pharmazeuten, Universitäts-Krankenhaus Eppendorf, Hamburg, Germany